UNCLASSIFIED

AD NUMBER

AD457746

NEW LIMITATION CHANGE

TO

Approved for public release, distribution unlimited

FROM

Distribution authorized to U.S. Gov't. agencies and their contractors; Administrative/Operational Use; 2 Feb 1965. Other requests shall be referred to U.S. Naval Civil Engineering Laboratory, Fort Hueneme, CA 93041.

AUTHORITY

USNCEL ltr, 21 Feb 1967

THIS PAGE IS UNCLASSIFIED

DASA — 11.026

R 354

Technical Report

FAST NEUTRON STREAMING THROUGH TWO-LEGGED CONCRETE DUCTS

2 February 1965

U. S. NAVAL CIVIL ENGINEERING LABORATORY
Port Hueneme, California

FAST NEUTRON STREAMING THROUGH TWO-LEGGED CONCRETE DUCTS

Y-F008-08-05-201, DASA-11.026

Type C

by

Y. T. Song

ABSTRACT

As a part of the Laboratory's fundamental shielding studies for personnel shelters, fast neutron dose rates are calculated in the second leg of an air duct through concrete for neutron energies of 14 Mev and 2.5 Mev. The calculational technique is based on the albedo concept. Dose rates are also calculated by a Monte Carlo technique, and the results obtained by the two theoretical methods are compared with each other and with experimental measurements.

Comparison shows very good agreement among these three independent determinations.

CONTENTS

INTRODUCTION

An important problem in shelter shielding is the streaming of fast neutrons through the shelter entranceway. Tentative experimental measurements have been made of fast neutron dose distributions in a duct,[1] but a theory for calculating the dose remains to be developed.

The problem of fast neutron streaming through ducts is different in many respects from the problem of deep penetration of neutrons within a medium. In the case of deep penetration, the interaction of the neutron with nuclei of the transporting medium is important. However, for the duct streaming problem, the principal factor is the reflection of neutrons from the walls of the duct. For deep penetration, then, the scattering medium can be treated as homogeneous; whereas in the duct streaming problem the material of which the walls are built and the material with which the duct is filled must be treated separately. In this study we shall be concerned with air ducts through concrete.

Because of the difference in nature between neutron streaming and deep penetration, the Boltzmann transport equation, which describes the deep penetration problem, cannot be used for the duct streaming problem. Therefore, special methods have been devised for treatment of the case of a cylindrical duct.[2] Since the geometry is more complicated for a rectangular duct than for a cylindrical one, the analytical approach has usually been abandoned in favor of Monte Carlo techniques in treatments of rectangular ducts. In this paper an analytical approach, using the albedo concept, will be applied to rectangular ducts.

In shielding calculations it is often preferable to be concerned with neutron dose instead of neutron flux, because biological hazard is more readily determined in terms of dose.* Moreover, calculational techniques are frequently simpler when dose is considered instead of flux. Note, for example, that neutron flux depends upon neutron energy as well as the angular and spatial variables, while dose, being proportional to integrated energy flux, depends only on the angular and spatial variables.

In order to formulate the equation which describes the variation of dose within a duct, it is necessary to know the differential dose albedo of neutrons striking the wall of the duct.

---

* I.e., absorbed, or rad, dose. Hereafter all references to dose will be to absorbed dose, unless otherwise specified.

In the next section, a formula for neutron albedo will be discussed. Following that, the albedo method will be used for calculating dose within a duct. Next, dose determinations by a Monte Carlo calculation and by experimental measurement will be discussed. Finally, the results obtained by these three independent methods will be compared.

SEMIEMPIRICAL FORMULA FOR NEUTRON DOSE ALBEDO

Definition of Albedo

The dose albedo for neutrons is defined as the ratio of the dose reflected from an area to the dose which is incident on the reflecting area. Because of the near equivalence between dose and the energy flux, an alternative definition is the ratio of the energy flux reflected from an area to the energy flux which is incident on the reflecting area. The definition of albedo as a ratio, as given above, is a conventional definition for total dose albedo.

In detailed shielding calculations, it is frequently necessary to know differential angular dose. Therefore, it is important to know the differential dose albedo. This is the ratio of the dose reflected per unit solid angle into the given direction from a differential area dA to the dose incident on surface area dA, as shown in Figure 1. Mathematically, differential dose albedo is expressed as

$$\alpha(E_o, \theta_o, \theta, \phi) = \frac{1}{D_o \cos\theta_o} \left(\frac{dD}{dA}\right)$$

where E_o = energy of incident neutron

θ_o = polar angle of incidence of neutron

θ = polar angle of reflected neutron

ϕ = azimuthal angle of reflected neutron

D = reflected dose rate

D_o = dose rate due to the incident neutron beam

The definition given above corresponds to that given by Chilton and Huddleston[3] for gamma-ray differential dose albedo.

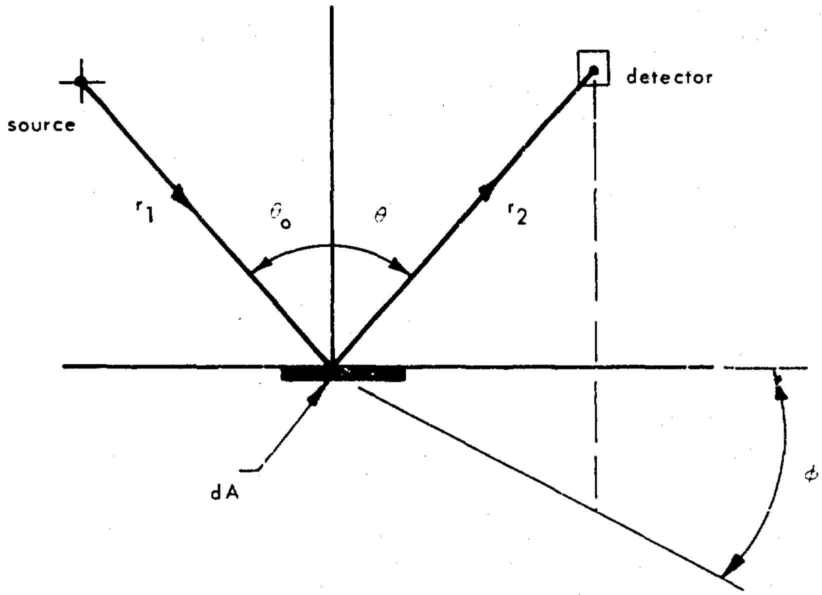

Figure 1. Reflection of neutron from a slab.

Frank J. Allen et al[4] have given the results of Monte Carlo calculations of neutrons backscattered from a semi-infinite slab of concrete. An attempt is made below to devise a semiempirical formula for the differential dose albedo of neutrons which will fit their Monte Carlo results.

Derivation of Formula

In the derivation of the desired semiempirical formula the following assumptions are made:

1. The energy dependence and the spatial dependence of the function describing the reflected neutron flux can be separated into an energy component and a spatial component, as follows:

$$n(E_o, \vec{r}, \vec{\Omega}) = N(E_o)\, \eta(\vec{r}, \vec{\Omega})$$

2. The scattering of neutrons in concrete is isotropic in the laboratory system. (Clearly, this assumption is not valid for fast neutrons or for elastic scattering of neutrons by light nuclei. However, it may be essentially valid for neutron scattering in concrete.)

3. The angular distribution of the reflected neutron dose is dominated by singly scattered neutrons. The scattered neutrons of the highest energy will be those which have been singly scattered. Of course, the multiple scattered neutrons also contribute to the reflected dose. However, it is assumed that the contribution from the singly scattered neutrons is much higher than the contribution of the multiple scattered neutrons. (Admittedly, this assumption is a weak point in the argument, its justification consisting mainly of the fact that correct answers are obtained to the problem at hand.) The neutron dose can be separated into a few components, such as a singly scattered part, and a multiple scattered part. However, for simplicity, only the singly scattered part is considered in this paper.

4. Neutron dose is approximately proportional to neutron energy flux. (This is a valid assumption for fast neutrons. For neutrons in the resonance energy region, the assumption is poor.)

Consider now a neutron scattering within a differential volume element dV which has a unit cross-sectional area and thickness dx at a slant depth x below the surface of a concrete slab, as shown in Figure 2. The probability of a neutron traversing without the interaction the distance inward to the volume element dV can be expressed as

$$e^{-\Sigma_t(E_o)x}$$

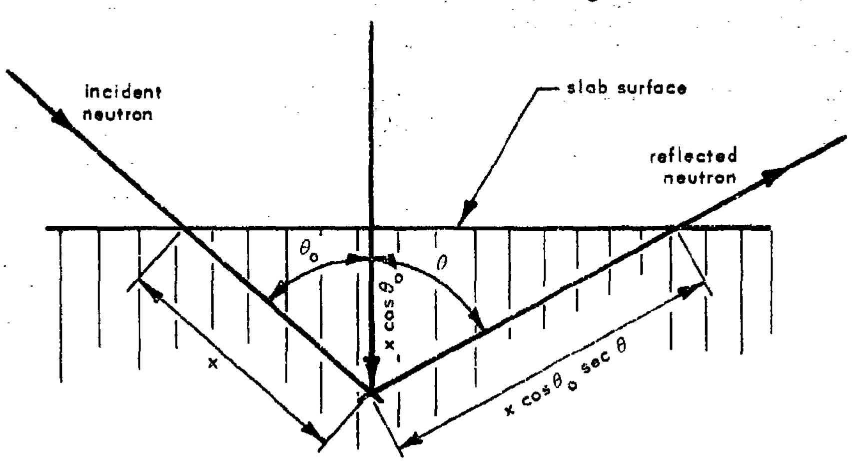

Figure 2. Simple scattering model of neutron in a slab.

On the assumption that the scattering is isotropic, the probability of a neutron traversing without interaction the distance from dV to the surface, after scatter, is proportional to

$$e^{-\Sigma_t(E_1)\,x\,\cos\theta_o\,\sec\theta}$$

where $\Sigma_t(E)$ = macroscopic total cross section

E_1 = energy of backscattering neutrons

Thus, the probability for a neutron to traverse a distance x into the scattering medium and then to be scattered back out of the surface is

$$\frac{1}{4\pi}\,\Sigma_s(E_o)\,e^{-\Sigma_t(E_o)x}\,e^{-\Sigma_t(E_1)\,x\,\cos\theta_o\,\sec\theta}$$

where Σ_s is the macroscopic scattering cross section.

Integrating over x from zero to infinity, in order to have all the singly scattered components,

$$\int_0^{\infty} e^{-\Sigma_t(E_o)x}\,e^{-\Sigma_t(E_1)\,x\,\cos\theta_o\,\sec\theta}\,dx$$

$$= \frac{1}{\Sigma_t(E_o) + \Sigma_t(E_1)\cos\theta_o\sec\theta}$$

On the assumption that $\Sigma_t(E_o) \approx \Sigma_t(E_1)$, the above equation can be written as

$$\frac{\frac{1}{4\pi}\Sigma_s(E_o)}{\Sigma_t(E_o) + \Sigma_t(E_1)\cos\theta_o\sec\theta} \approx \frac{\frac{1}{4\pi}\Sigma_s(E_o)}{\Sigma_t(E_o)\,(1 + \cos\theta_o\sec\theta)}$$

$$\approx \frac{A(E_o)}{1 + \cos\theta_o\sec\theta}$$

where $A(E_o)$ is an energy-dependent parameter, equivalent to $(1/4\pi)[\Sigma_s(E_o)/\Sigma_t(E_o)]$. But $A(E_o)/1 + \cos\theta_o \sec\theta$ is just the probability per unit solid angle per unit area normal to its direction of motion that a neutron incident at θ_o scatters in the direction θ. Therefore, the differential dose albedo for neutrons can be written as

$$\alpha(E_o, \theta_o, \theta) = \frac{A(E_o)\cos\theta}{\cos\theta_o + \cos\theta} \tag{1}$$

It is not necessary to specify the azimuthal dependence of albedo since the assumption was made that the scattering was isotropic in the laboratory system.

Values for the energy-dependent parameter $A(E_o)$ were obtained for each of the incident neutron energies (0.1, 0.25, 0.5, 1, 2, 3, 5, and 14 Mev) by means of a least-squares analysis to provide the best fit of the above equation to the Monte Carlo data of Allen.[4]

In Allen's data, the dose reflection factor per steradian (DRF) is defined as

$$(DRF)_j = \frac{\sec\theta_j}{D\Omega_j} \sum_{i=1}^{10} R_{ij} D_i \quad ; \quad j = 1, 2, \ldots 12$$

where subscripts i and j refer to the ith energy group and the jth angular sector. The terms are

θ = polar angle of reflection

Ω = solid angle of sector

D = incident dose per neutron

R = reflection factor

The angular sectors used by Allen are shown in Tables I and II. Table I shows the angular sectors, average reflection angle, and solid angle of each sector for the case of normal incidence. The average reflection angle of a sector, θ, is the arithmetic mean of the polar angles of the two end points, θ_1 and θ_2, of the sector. For the case of normal incidence, there is no azimuthal dependence for the sectors.

Table I. Angular Sector Histogram for Normal Incidence ($\cos\theta_o = 1$)

Sector	$\bar{\theta}$	θ_1	θ_2	Solid Angle
1	$8^\circ 18'$	0	$16^\circ 35.9'$	0.2618
2	$20^\circ 5'$	$16^\circ 35.9'$	$23^\circ 33.4'$	0.2618
3	$26^\circ 45'$	$23^\circ 33.4'$	$29^\circ 55.6'$	0.31416
4	$32^\circ 35'$	$29^\circ 55.6'$	$35^\circ 14.8'$	0.31416
5	$37^\circ 36'$	$35^\circ 14.8'$	$39^\circ 56.7'$	0.31416
6	$42^\circ 5'$	$39^\circ 56.7'$	$44^\circ 13.2'$	0.31416
7	$46^\circ 12'$	$44^\circ 13.2'$	$48^\circ 11.4'$	0.31416
8	$51^\circ 15'$	$48^\circ 11.4'$	$54^\circ 18.9'$	0.52360
9	$57^\circ 9'$	$54^\circ 18.9'$	$60^\circ 0'$	0.52360
10	$62^\circ 41'$	$60^\circ 0'$	$65^\circ 22.5'$	0.52360
11	$67^\circ 57'$	$65^\circ 22.5'$	$70^\circ 31.7'$	0.52360
12	$80^\circ 16'$	$70^\circ 31.7'$	90°	2.0944

Table II. Angular Sector Histogram for Slant Incidence

Sector	$\overline{\theta}$	θ_1	θ_2	ϕ_1	ϕ_2	Solid Angle
1	11°47'	0	23°33.4'	0	π	$\pi/6$
2	35°52'	23°33.4'	48°11.4'	$2\pi/3$	π	$\pi/6$
3	35°52'	23°33.4'	48°11.4'	$\pi/3$	$2\pi/3$	$\pi/6$
4	35°52'	23°33.4'	48°11.4'	0	$\pi/3$	$\pi/6$
5	59°22'	48°11.4'	70°31.7'	$3\pi/4$	π	$\pi/6$
6	59°22'	48°11.4'	70°31.7'	$\pi/2$	$3\pi/4$	$\pi/6$
7	59°22'	48°11.4'	70°31.7'	$\pi/4$	$\pi/2$	$\pi/6$
8	59°22'	48°11.4'	70°31.7'	0	$\pi/4$	$\pi/6$
9	80°16'	70°31.7'	90°	$3\pi/4$	π	$\pi/6$
10	80°16'	70°31.7'	90°	$\pi/2$	$3\pi/4$	$\pi/6$
11	80°16'	70°31.7'	90°	$\pi/4$	$\pi/2$	$\pi/6$
12	80°16'	70°31.7'	90°	0	$\pi/4$	$\pi/6$

Table II shows the angular sector histogram for the case of slant incidence. The average polar angle, $\overline{\theta}$, is obtained in the same manner as for Table I. The angles ϕ_1 and ϕ_2 are the end points of the azimuthal angles for each section.

Since the dose reflection factor computed by Allen is not the same as the term $\alpha\ (E_o, \theta_o, \theta)$ as used in this report, his values must be converted by the relationship

$$\alpha_j = \frac{(DRF)_j \cos\theta_j}{\cos\theta_o}$$

As there appears to be no significant variation of α with ϕ, the azimuthal dependence of albedo is neglected throughout this report.

The least-squares analysis was carried out on the Laboratory's IBM-1620. The values thus obtained for $A\,(E_o)$ are shown in Table III and in Figure 3.

Until now, $A\,(E_o)$ has been treated as an empirical energy-dependent parameter. It has been observed that the curve for $A\,(E_o)$ as a function of E_o can be fitted by a least-squares regression analysis to the formula

$$A\,(E_o) = E_o\, e^{a + b\sqrt{E_o} + cE_o}$$

where $a = 0.9719$

$b = -2.895$

$c = 0.3417$

The equation for differential dose albedo can now be written, semiemperically, as

$$\alpha\ (E_o, \theta_o, \theta) = \frac{E_o \cos\theta}{\cos\theta_o + \cos\theta}\, e^{0.9719 - 2.895\sqrt{E_o} + 0.3417\,E_o} \qquad (2)$$

Comparisons between the one-parameter formula (Equation 1), the semiempirical formula (Equation 2), and Allen's Monte Carlo results are shown in the Appendix.

Table III. Values of Energy-Dependent Parameter for One-Parameter Semiempirical Formula for Differential Neutron Dose Albedo on Concrete

$A(E_o)$	E_o (Mev)
0.146	0.1
0.154	0.25
0.157	0.5
0.192	1.0
0.173	2.0
0.155	3.0
0.127	5.0
0.084	14.0

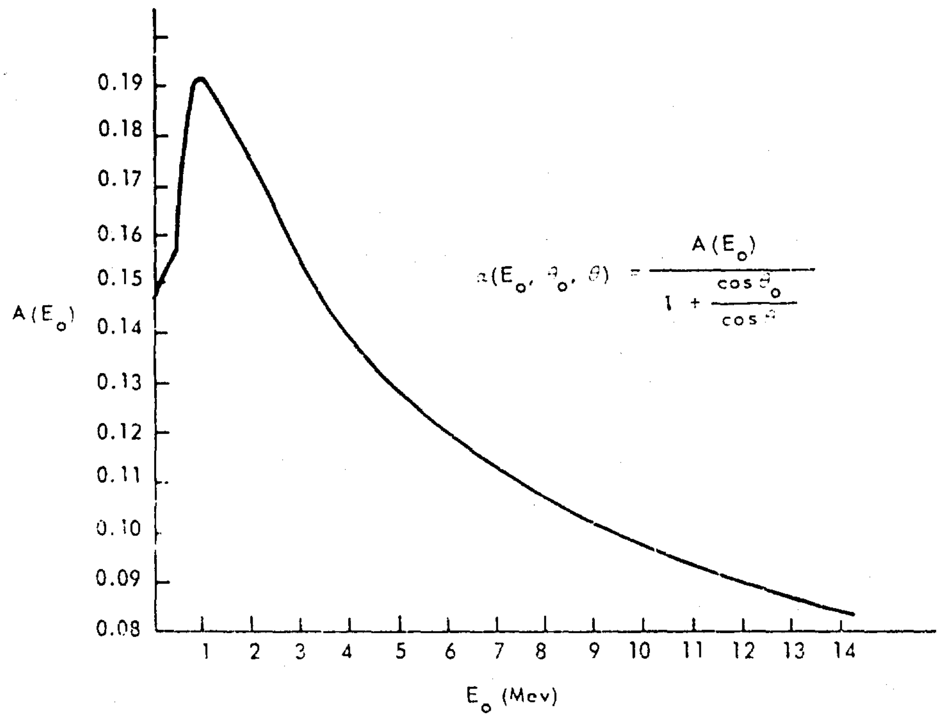

Figure 3. Graph of values obtained for $A(E_o)$ listed in Table III.

CALCULATION OF DOSE IN A DUCT

On the basis of the formula for differential dose albedo just derived, it is possible to develop an expression governing neutron dose distribution within a duct.*

First, consider the most general problem of neutron transport through a medium. The Boltzmann type transport equation is regarded as the complete relation for neutron, or radiation, transport. However, the transport equation cannot be easily solved for the duct problem because of the complexity of the geometry and physics involved. The steady-state neutron transport equation can be written, in the integral form,[5] as

$$n(\vec{r}, \vec{\Omega}, v) = \int\int\int dV \int\int\int n(\vec{r}', \vec{\Omega}', v') K(\vec{r}', \vec{\Omega}', v' \rightarrow \vec{r}, \vec{\Omega}, v)\, dv'\, d\Omega' + S_o \qquad (3)$$

where

$n(\vec{r}, \vec{\Omega}, v)$ = mean number of neutrons per unit volume per unit solid angle per unit velocity interval at position r, with scaler velocity v in the direction of Ω

$K(\vec{r}', \vec{\Omega}', v' \rightarrow \vec{r}, \vec{\Omega}, v)$ = probability per unit volume that a neutron described by the coordinates $\vec{r}'$, $\vec{\Omega}'$, and v' is scattered such that the new coordinates are r, $\vec{\Omega}$, and v

dV = differential volume

S_o = source term = mean number of unscattered neutrons from source reaching $\vec{r}$, with scaler velocity v in the direction $\vec{\Omega}$, per unit volume per unit solid angle per unit velocity interval

* Gamma-ray dose distribution calculated by the albedo model, using a method very similar to the one developed in this study, gives very good agreement with experimental results, as discussed by Chapman.[6]

Changing the variable from scaler velocity v to energy E, the angular neutron energy flux can be written as $E n (E, \vec{r}, \vec{\Omega})$. Therefore, neutron dose, D, can be expressed as the angular dependent quantity:

$$D(\vec{r}, \vec{\Omega}) = \int_{o}^{E_{max}} f(E) E n (E, \vec{r}, \vec{\Omega}) dE$$

where E_{max} is the maximum neutron energy, and f (E) is the energy-dependent response function for neutron dose. In the monoenergetic case, the above expression reduces to

$$D(\vec{r}, \vec{\Omega}) = f(E) E n (\vec{r}, \vec{\Omega})$$

In order to obtain the dose transport equation, multiply Equation 3 by E f (E) and change the variable from v to E. This gives

$$n(E, \vec{r}, \vec{\Omega}) E f(E) = \int\int\int dV \int\int\int \frac{E f(E) K(E', \vec{\Omega}', \vec{r}' \rightarrow E, \vec{r}, \vec{\Omega})}{E' f(E')} \cdot$$

$$n(E', \vec{r}', \vec{\Omega}') E' f(E') dE' d\Omega' + S_o E f(E)$$

Integration over energy space gives angular dose, $D(\vec{r}, \vec{\Omega})$, due to the angular neutron energy flux:

$$D(\vec{r}, \vec{\Omega}) = \int\int\int dV \int\int\int D(\vec{r}', \vec{\Omega}') \frac{E f(E) K(E', \vec{\Omega}', \vec{r}' - E, \vec{r}, \vec{\Omega})}{E' f(E')} dE d\Omega'$$

$$+ D_s (\vec{r}, \vec{\Omega})$$

where D_s is the dose due to the uncollided angular neutron energy flux from the source.

This equation can be written as

$$D(\vec{r}, \vec{\Omega}) = \int\int\int dV \int\int k(\vec{r}', \vec{\Omega}' \rightarrow \vec{r}, \vec{\Omega}) D(\vec{r}', \vec{\Omega}') d\Omega' + D_s(\vec{r}, \vec{\Omega})$$

where $k(\vec{r}', \vec{\Omega}' \rightarrow \vec{r}, \vec{\Omega})$ is the dose transport kernel and

$$k(\vec{r}', \vec{\Omega}' \rightarrow \vec{r}, \vec{\Omega}) = \int \frac{E f(E) K(E', \vec{\Omega}', \vec{r}' \rightarrow E, \vec{r}, \vec{\Omega})}{E' f(E')} dE$$

For the duct problem, our concern is not with the transport medium but with reflection from the walls of the duct. In this case, the dose transport equation can, by analogy, be written as

$$D(\vec{r}, \vec{\Omega}) = \int_{\Omega'} \int_{Area} D(\vec{r}', \vec{\Omega}') \chi(\vec{r}', \vec{\Omega}' \rightarrow \vec{r}, \vec{\Omega}) dA \, d\Omega' + D_s(\vec{r}, \vec{\Omega}) \qquad (4)$$

where integration is carried out over the reflecting surface, A (the floor, ceiling, and walls of the duct). In this case, the kernel $\chi(\vec{r}', \vec{\Omega}' \rightarrow \vec{r}, \vec{\Omega})$ has a different meaning. It is the probability that the angular energy flux which corresponds to $D(\vec{r}', \vec{\Omega}')$ is reflected at differential area dA such that it becomes $D(\vec{r}, \vec{\Omega})$. $D_s(\vec{r}, \vec{\Omega})$ is the uncollided dose contribution from the source.

Consider the difference between Equation 3 and Equation 4. In Equation 3 the quantity of interest is the neutron flux as a function of angle, position, and velocity. Therefore, the entire range of neutron energy is important. However, in Equation 4 the important quantity is the neutron dose integrated over energy.

For the same value of $n(E, \vec{r}, \vec{\Omega})$ per unit energy interval, $En(E, \vec{r}, \vec{\Omega})$ always has a relatively higher value in the high energy range. Furthermore, the response function for neutron dose, f(E), has higher values for higher neutron energies. Therefore, as far as the total neutron dose is concerned, the lower energy neutron contribution is much less than the higher energy neutron contribution if there is roughly the same neutron density at all energies.

Now, during the slowing-down process of a neutron, while it is streaming through the duct by reflection from the walls, the more reflections there are from the wall, the more the neutron loses its energy, until it is slowed down to thermal energy. The result of this slowing-down process can be expressed in simple mathematical form.

Let I_i be the neutron dose contributed by the ith reflection:

$$I_i(\vec{r}, \vec{\Omega}) = \int_{\substack{\text{Solid} \\ \text{angle}}} \int_{\text{Area}} I_{i-1}(\vec{r'}, \vec{\Omega}) \varkappa (\vec{r'}, \vec{\Omega}' \rightarrow \vec{r}, \vec{\Omega}) \, dA \, d\Omega'$$

$$I_o(\vec{r}, \vec{\Omega}) = D_s(\vec{r}, \vec{\Omega})$$

Since neutrons contributing to I_i have been scattered at least i times, and since each scatter results in a degradation in energy,

$$I_i(\vec{r}, \vec{\Omega}) > I_{i+1}(\vec{r}, \vec{\Omega}) \tag{5}$$

Next, consider the geometrical factor for neutron reflection which affects the total dose in a duct. For simplicity, consider a straight cylindrical duct as shown in the following diagram.

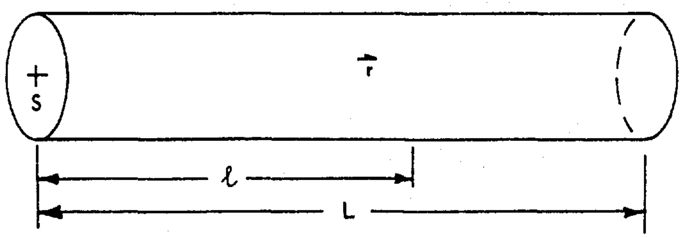

The source is placed on the centerline at the entrance to the duct. The detector is at r. The total reflection area is $2\pi RL$, where R is the radius of the duct, and L is the total length of the duct. Then the dose at $\vec{r}$ is

$$D(\vec{r}, \vec{\Omega}) = \int_{\substack{\text{Solid}\\ \text{angle}}} \int_{\text{Area}} D(\vec{r}', \vec{\Omega}')\, \chi(\vec{r}', \vec{\Omega}' \rightarrow \vec{r}, \vec{\Omega})\, dA\, d\Omega' + D_s(\vec{r}, \vec{\Omega}) \tag{6}$$

Letting ℓ be the axial distance from source to detector, Equation 6 can be written as

$$D(\vec{r}, \vec{\Omega}) = \int_{\substack{\text{Solid}\\ \text{angle}}} \int_{L=0}^{L=\ell} D(\vec{r}', \vec{\Omega}')\, \chi(\vec{r}', \vec{\Omega}' \rightarrow \vec{r}, \vec{\Omega})\, d\Omega'\, 2\pi R\, d\ell$$

$$+ \int_{\substack{\text{Solid}\\ \text{angle}}} \int_{\ell}^{L} D(\vec{r}'', \vec{\Omega}'')\, \chi(\vec{r}'', \vec{\Omega}'' \rightarrow \vec{r}, \vec{\Omega})\, d\Omega''\, 2\pi R\, d\ell + D_s(\vec{r}, \vec{\Omega}) \tag{7}$$

Now, for certain values of ℓ, the second term of Equation 7 is smaller than the first terms for two reasons. (1) The distances between the source and the detector are greater. (2) At larger distances, higher orders of reflection are more likely relative to the number of low-order reflections.

In view of the above considerations, the first approximation to the solution of Equation 4 can be written as

$$D_1(\vec{r}, \vec{\Omega}) = D_s(\vec{r}, \vec{\Omega}) \tag{8}$$

The second approximation is

$$D_2(\vec{r}, \vec{\Omega}) \int_{\substack{\text{Solid}\\ \text{angle}}} \int_{\text{Area}} D_1(\vec{r}', \vec{\Omega}')\, \chi(\vec{r}', \vec{\Omega}' \rightarrow \vec{r}, \vec{\Omega})\, dA\, d\Omega' + D_s(\vec{r}, \vec{\Omega}) \tag{9}$$

The third approximation is

$$D_3(\vec{r}, \vec{\Omega}) = \int_{\substack{\text{Solid}\\\text{angle}}} \int_{\text{Area}} D_2(\vec{r'}, \vec{\Omega'})\, \varkappa(\vec{r'}, \vec{\Omega'} \rightarrow \vec{r}, \vec{\Omega})\, dA\, d\Omega' + D_s(\vec{r}, \vec{\Omega}) \quad (10)$$

The solution of Equation 4 can then be written as

$$D(\vec{r}, \vec{\Omega}) \doteq D_n(\vec{r}, \vec{\Omega}) = \sum_{i=0}^{n} I_i(\vec{r}, \vec{\Omega}) \quad (11)$$

where $I_o(\vec{r}, \vec{\Omega})$ corresponds to $D_s(\vec{r}, \vec{\Omega})$.

Since $I_i(\vec{r}, \vec{\Omega}) > I_{i+1}(\vec{r}, \vec{\Omega})$, as previously discussed, the series approximation of the solution of Equation 4 must converge under all circumstances because $D_n(\vec{r}, \vec{\Omega})$ is bounded by the source strength for all n.

Equation 4 can be applied directly to the two-legged rectangular concrete duct problem. The dose transport kernel is

$$\varkappa(\vec{r'}, \vec{\Omega'} \rightarrow \vec{r'}, \vec{\Omega'}) = \frac{1}{R_1^{\,2} R_2^{\,2}}\, \alpha(E_o, \theta_o, \theta) \cos\theta_o$$

where R_1 = distance from source to the reflecting area, dA

R_2 = distance from dA to the detector

$\cos\theta_o$ = cosine of the polar angle from the source dA

$\alpha(E_o, \theta_o, \theta)$ = differential dose albedo

In the second leg of the two-legged duct, the source function of Equation 4 drops out if the detector in the second leg cannot see the source directly. Then

$$D(\vec{r}, \vec{\Omega}) = \sum_{i=1}^{n} I_i(\vec{r}, \vec{\Omega})$$

Now, for the singly reflected neutron dose, $I_1(\vec{r}, \vec{\Omega})$ can be written as

$$I_1(\vec{r}, \vec{\Omega}) = \int_{\substack{\text{Solid}\\\text{angle}}} \int_{\text{Area}} \frac{D_o \cos\theta_o}{R_1^2 R_2^2} \alpha(E_o, \theta_o, \theta)\, dA\, d\Omega \tag{12}$$

where D_o is the dose at unit distance from the source in air.

The doubly reflected neutron dose is

$$I_2(\vec{r}, \vec{\Omega}) = \int_{\substack{\text{Solid}\\\text{angle}}} \int_{\text{Area}} I_1(\vec{r}', \vec{\Omega}') \frac{\cos\theta_o}{R_1^2 R_2^2} \alpha(E_1, \theta_o, \theta)\, dA\, d\Omega' \tag{13}$$

where R_1 = distance from the first reflecting area to the second reflecting area, dA

R_2 = distance from dA to the detector

$\cos\theta_o$ = cosine of the polar angle from the first reflecting area to dA

$\alpha(E_1, \theta_o, \theta)$ = differential dose albedo of singly reflected neutrons

In the same way, the neutron dose from the higher orders of reflection can be obtained.

The general formula, Equation 4, is based on neutron reflection. However, there are a certain number of neutrons which penetrate the corner lip of the duct and are reflected to the detector. Also, corner-lip scattering of neutrons contributes to the total dose in the second leg of the duct. Therefore, these factors have to be taken into account for the total dose in a duct with a bend.

The calculation of $D(\vec{r}, \vec{\Omega})$ was carried out by the IBM-1620 computer. The details of the calculation are discussed in the following sections.

1. Calculation of Primary Reflection

Equation 12 is equivalent to the LeDoux-Chilton formula for calculating the contribution of the primary reflection to the gamma-ray dose in a two-legged rectangular duct.[7] In their calculation, the primary reflecting area was divided as shown in Figure 4, and R_1, R_2, θ_o, and θ were considered constant. For this calculation, the primary reflecting areas were divided into five sub-areas as shown in Figure 5, the source was considered to be at the mouth of the duct, and the detector was taken to be placed on the centerline of the second leg. The detector position coordinate was (x_d, y_d, o). Each sub-area was divided into m increments. The dose rate contributed by the reflection from each sub-area, ΔA, was calculated using the equation

$$D_j(\vec{r}, \vec{\Omega}) = \frac{D_o \alpha_j \cos\theta_{o_j} \Delta A_j}{R_{1_j}^{\,2} R_{2_j}^{\,2}} \qquad (14)$$

The dose rate due to primary reflection was obtained by

$$D_1(\vec{r}, \vec{\Omega}) = \sum_{j=1}^{m} D_j(\vec{r}, \vec{\Omega})$$

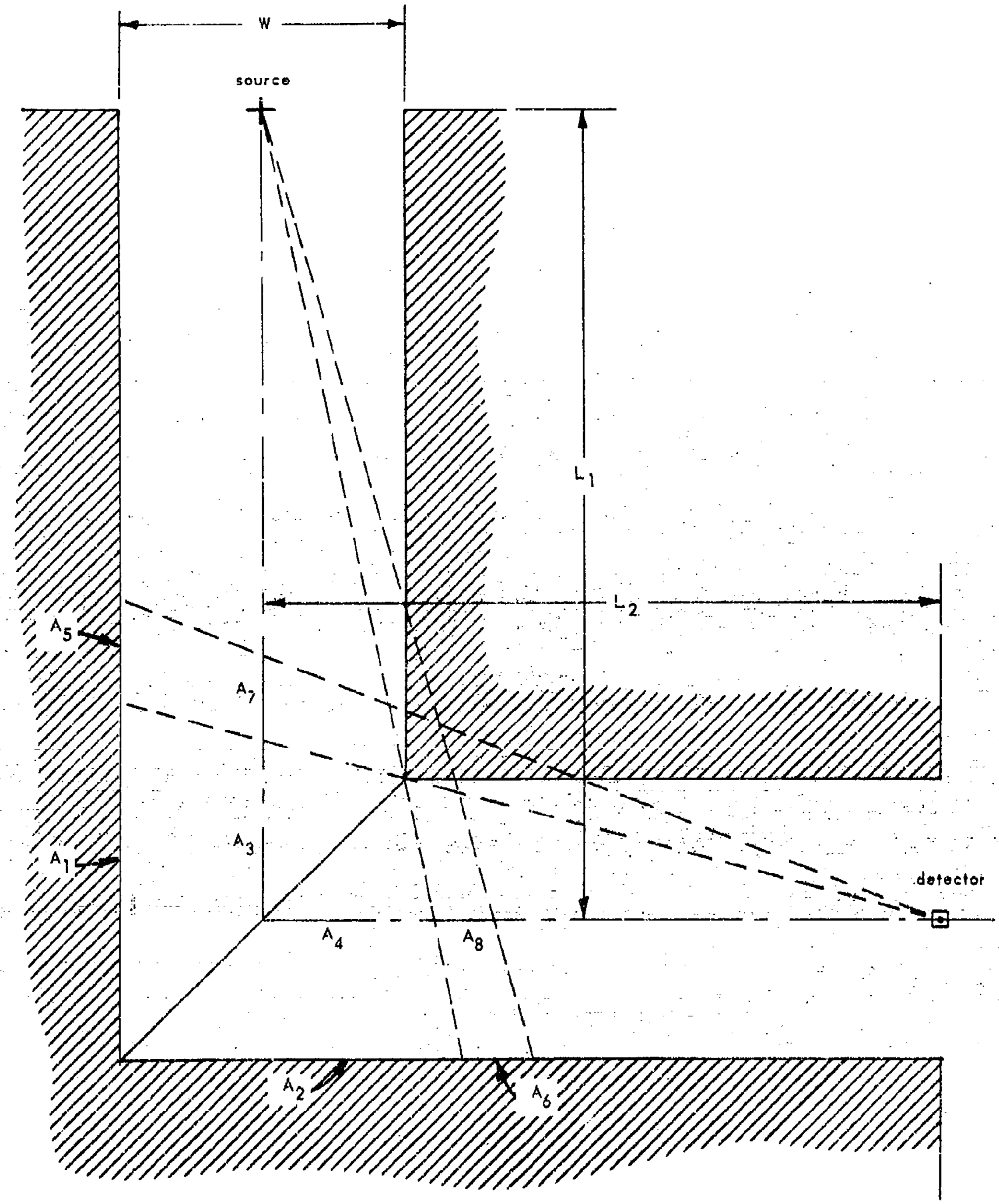

Figure 4. Duct geometry showing primary reflecting areas.

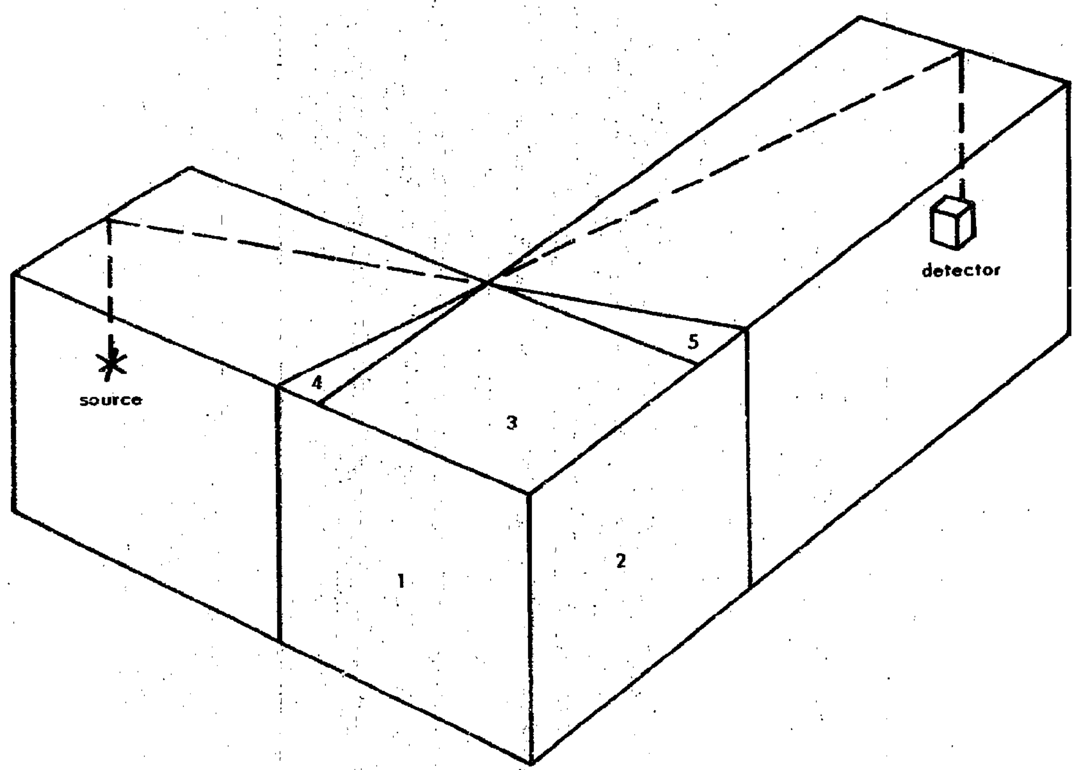

Figure 5. Division of primary reflecting areas for calculation by incremental areas.

2. Calculation of Secondary Reflection

Equation 13 was evaluated in the same way as Equation 12 was evaluated for primary reflection. The secondary reflecting area was divided as shown in Figure 6. The contribution of the secondary reflection was obtained by taking combinations of the scattering areas; for example, the combination of the source + 1 + 6 + D, or of the source + 2 + 5 + D. This time the scattering area was not divided into incremental areas, but the parameters were obtained for the center of each scattering area. This method is very similar to that of Chapman for calculating gamma-ray dose attenuation in two-legged ducts.[6]

The working equation for this secondary reflection is

$$D_{2_k}(\vec{r}, \vec{\Omega}) = \frac{D_o A_i A_i \cos\theta_{01} \cos\theta_{02} \alpha_1 \alpha_2}{R_1^2 R_2^2 R_3^2}$$

and

$$D_2(\vec{r}, \vec{\Omega}) = \sum_{k=1} D_{2_k}(\vec{r}, \vec{\Omega})$$

3. Corner Inscattering and Transmission

The corner inscattering and transmission contribution from the corner lip of the duct is discussed in great detail in Reference 7 for the gamma-ray case. For the neutron case, some modification is necessary because of the physical nature of the problem. The corner transmission is treated the same way as it was for the gamma-ray case. The treatment of corner inscattering, however, is based on the assumption that the scattering of neutrons in concrete is isotropic in the laboratory system. In this calculation, only the primary effect is considered for corner transmission; and for corner inscattering the primary and secondary effects are taken into consideration. For the secondary corner inscattering effect, only four special cases which seem to be important are considered. They are shown in Figure 7.

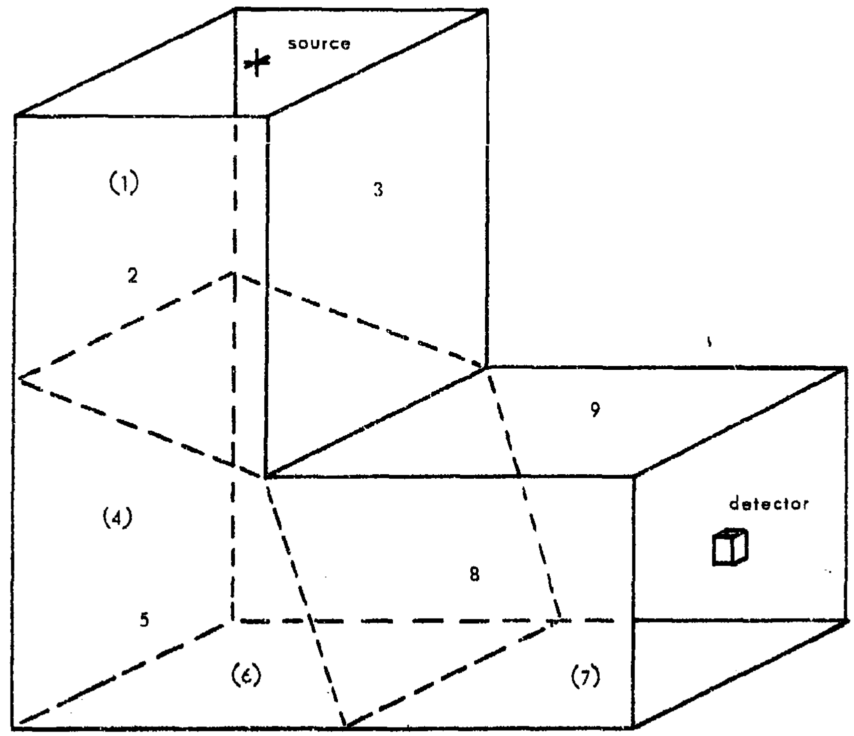

(a)

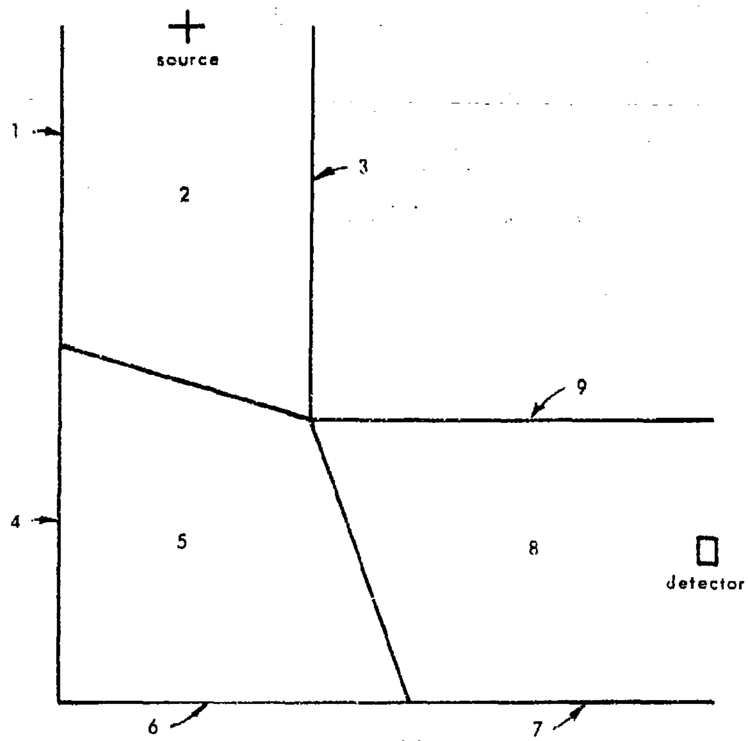

(b)

Figure 6. Division of secondary reflecting areas.

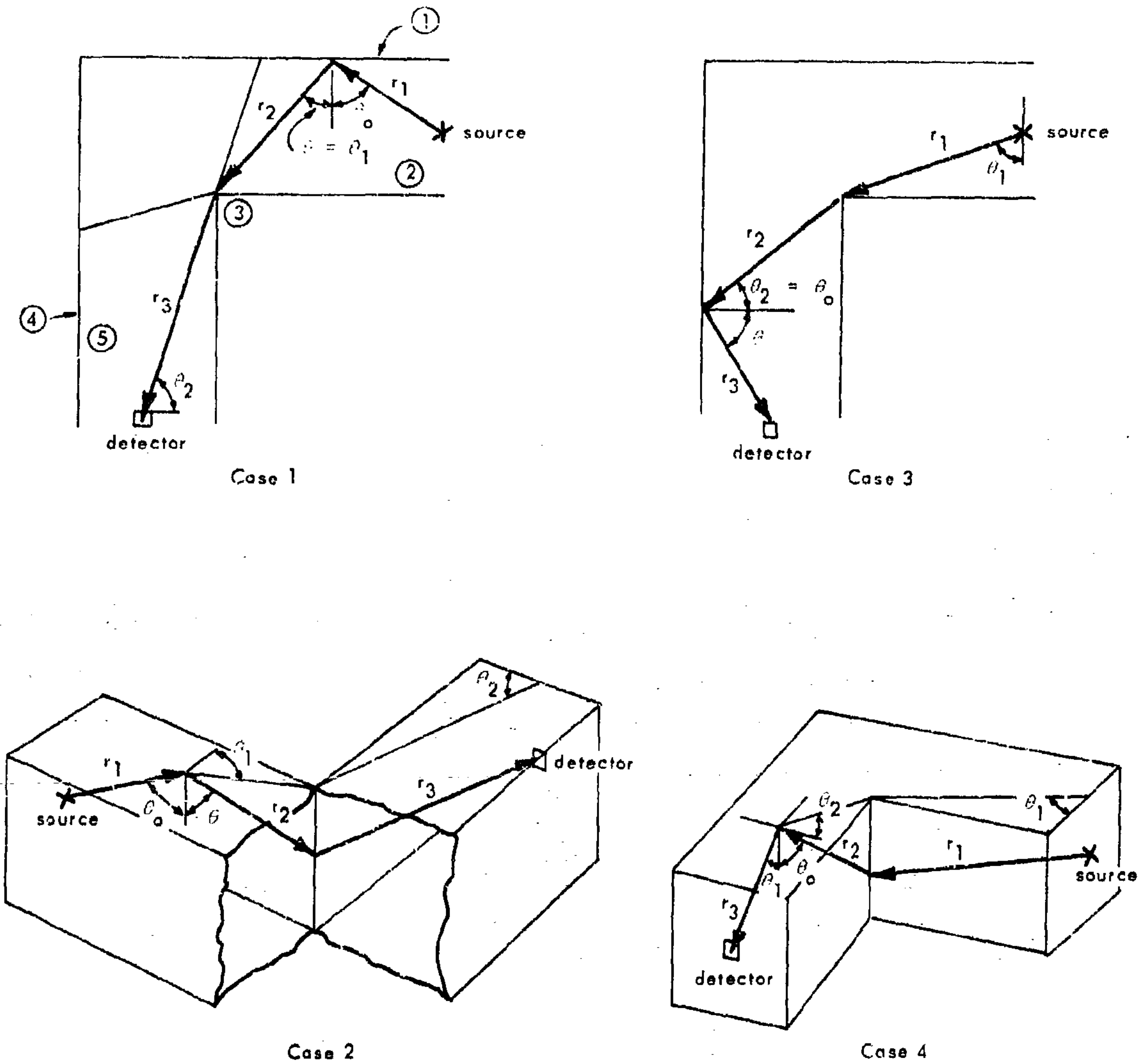

Figure 7. Geometry for multiple corner inscattering with scattering surface in the first leg (Cases 1 and 2) and in the second leg (Cases 3 and 4). Areas 2 and 5 in Case 1 are either ceiling or floor.

CALCULATION BY MONTE CARLO METHOD, USING ADONIS CODE[8]

One approach to the solution to the problem of neutron streaming through a duct is the Monte Carlo method. The ADONIS code solves the transport equation by the Monte Carlo method for neutrons traveling through a configuration consisting of a finite number of rectangular parallelepiped regions. ADONIS calculates the flux, F, in each region as follows:

$$F(r, j) = \frac{S(r, j)}{V_r}$$

where $S(r, j) = (1/E_j - E_{j-1}) [W(r)/Gn] \sum_{g=1}^{G} S_g(r, j)$

and $S_g(r, j)$ = track length of the gth group of neutrons in region r, with energy E satisfying $E_{j-1} \leq E \leq E_j$

V_r = volume of region r

G = total number of Monte Carlo groups

n = number of neutron histories per group

$W(r)$ = weighting factor for region r

The flux, as defined above, is the total track length per unit volume per unit energy interval. This gives the flux averaged over the volume of the region. In order to get the flux at any desired point, the volume of the region must be sufficiently small so that the flux averaged over the volume can represent the flux at the midpoint of the volume. If the volume of the region is small, the statistics are usually very poor unless the case history number is tremendously high. In order to overcome this difficulty, it is assumed that the flux over the cross-sectional area can be reasonably well represented at the center of that area.

ADONIS calculations based on this assumption are compared with albedo model calculations and experimental measurements following the next section.

EXPERIMENTAL MEASUREMENTS OF FAST NEUTRON DOSE DISTRIBUTIONS IN DUCTS

Some preliminary experiments have been carried out at NCEL by Doty.[1] Using a neutron generator, neutron sources with energies of 14 Mev and 2.5 Mev were obtained by T (d, n) and D (d, n) reactions. The dose rates were measured by a 12-inch spherical dosimeter in a 3 x 3-foot concrete duct. All the values measured by the dosimeter were normalized by a monitor value obtained with a paraffin-covered BF_3 counter at an arbitrary position. The results so obtained are reproduced in Figures 8 and 9.

In this experiment, only one duct size was used. Therefore, the shape dependency was not studied, but the dose distribution as a function of the distance from the intersection of the two legs was studied.

The dose rate fell off approximately as the inverse square of the distance along the axis of the firsr leg of the duct. In the second leg, the rate fell off more rapidly — approximately as the inverse third or fourth power of the distance along the axis of the leg. Note that this finding is different from the exponential dose attenuation that would be expected for deep penetration through a homogeneous medium.

Since dose rates are proportional to a power of axial distance, it seems clear that neutron penetration through duct walls is small compared with reflection from the walls. The above argument is true only when the thickness of the walls is greater than a mean free path of the initial neutrons.

COMPARISON BETWEEN EXPERIMENT, MONTE CARLO CALCULATIONS, AND ALBEDO CALCULATIONS

Experimental results for neutron dose were obtained from the spherical dosimeter in units of rem. But the dose calculated by the albedo model is given in rad units. Therefore, rad dose was converted to rem dose to allow direct comparison of theoretical results with experimental findings. In this procedure, the average energies of the singly reflected neutron and doubly reflected neutron were obtained by averaging Allen's Monte Carlo data[4] over the reflecting angle weighted by the number of neutrons in each reflecting angular sector. The energies thus obtained were used to convert rad dose calculated by the albedo model to rem dose according to the spherical dosimeter response (which is close to being tissue equivalent).[9]

In the same way, the results of ADONIS Monte Carlo calculations were converted from neutron flux to dose according to the spherical dosimeter response function.

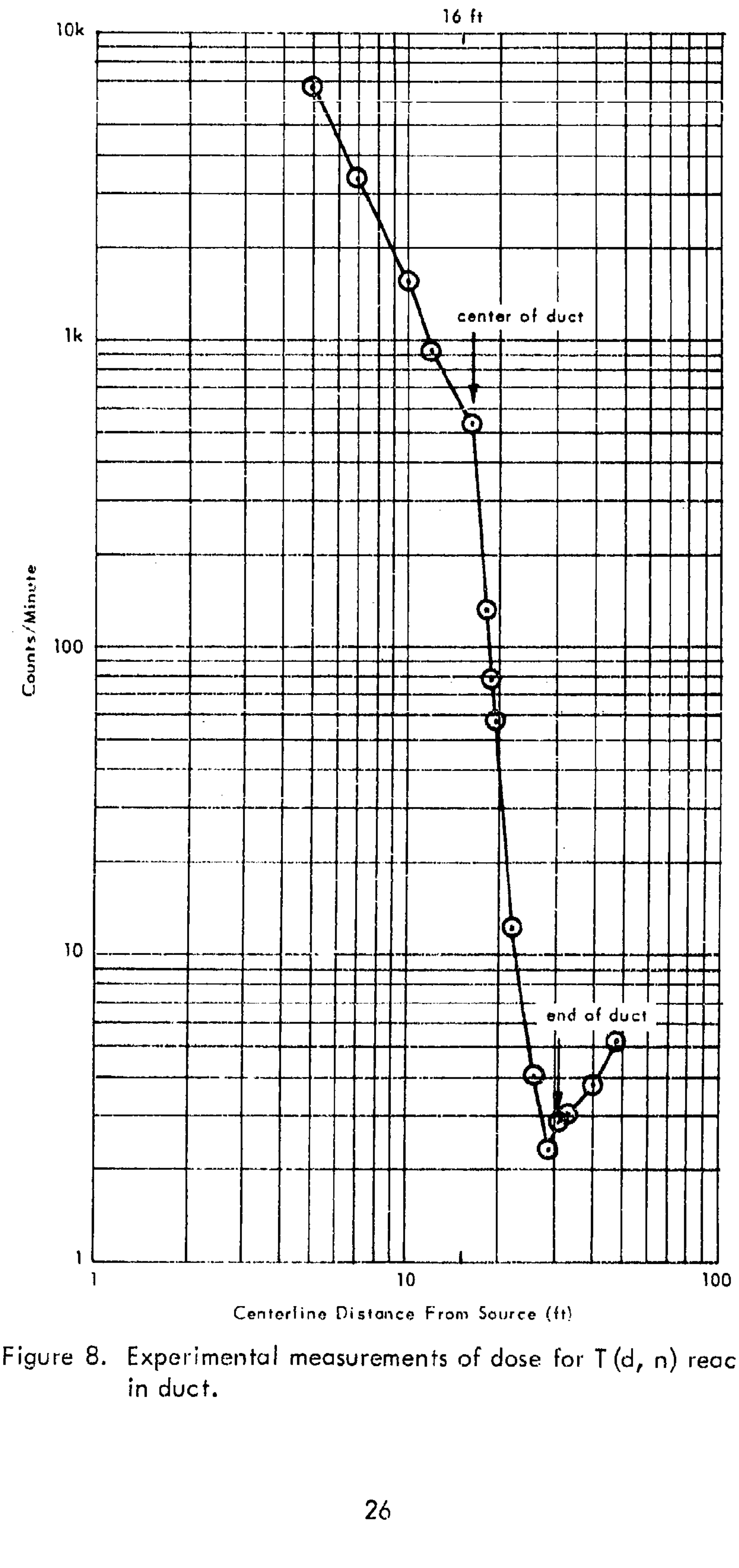

Figure 8. Experimental measurements of dose for T (d, n) reaction in duct.

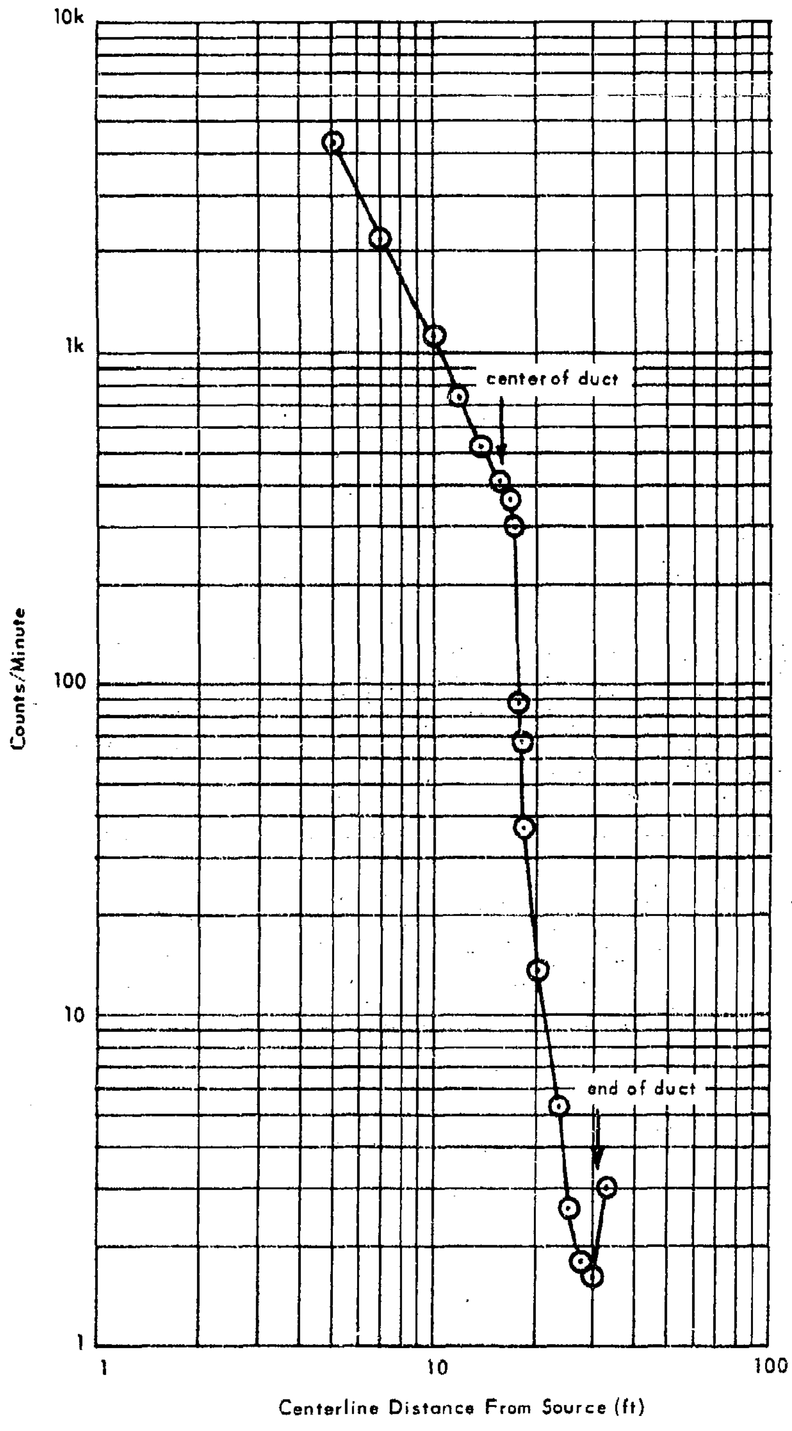

Figure 9. Experimental measurements of dose for D (d, n) reaction in duct.

In comparing the ADONIS results to others, in order to evaluate the representative value in a given region, the following technique is applied:

Let $(D/D_o)_{ADONIS}$ = results of the ratio of dose at detector to dose at unit distance from the source in air obtained by ADONIS in a given region

$(D/D_o)_x$ = results of the same ratio calculated by the albedo model at point x, which is in a region corresponding to the region specified by ADONIS

The mean value of D/D_o within a region extending from x_i to x_{i+1} and across the entire cross section of the duct is, by the Mean Value Theorem,

$$\overline{\left(\frac{D}{D_o}\right)} = \frac{\int_{x_i}^{x_{i+1}} \left(\frac{D}{D_o}\right)_x dx}{\int_{x_i}^{x_{i+1}} dx}$$

This mean value for D/D_o can be obtained by graphical integration of the values for $(D/D_o)_x$ obtained from albedo calculations.

Comparisons can now be made between $\overline{D/D_o}$ and $(D/D_o)_{ADONIS}$ for the region which extends from x_i to x_{i+1}. The comparison is made at the point $\overline{x}$ such that

$$\left(\frac{D}{D_o}\right)_{\overline{x}} = \overline{\left(\frac{D}{D_o}\right)}$$

The comparison is shown in Figure 10 for an 11-inch square duct. It is seen that the albedo model calculations give somewhat lower values than do the Monte Carlo calculations. This result is expected since orders of reflection higher than the second are neglected in the albedo model calculations.

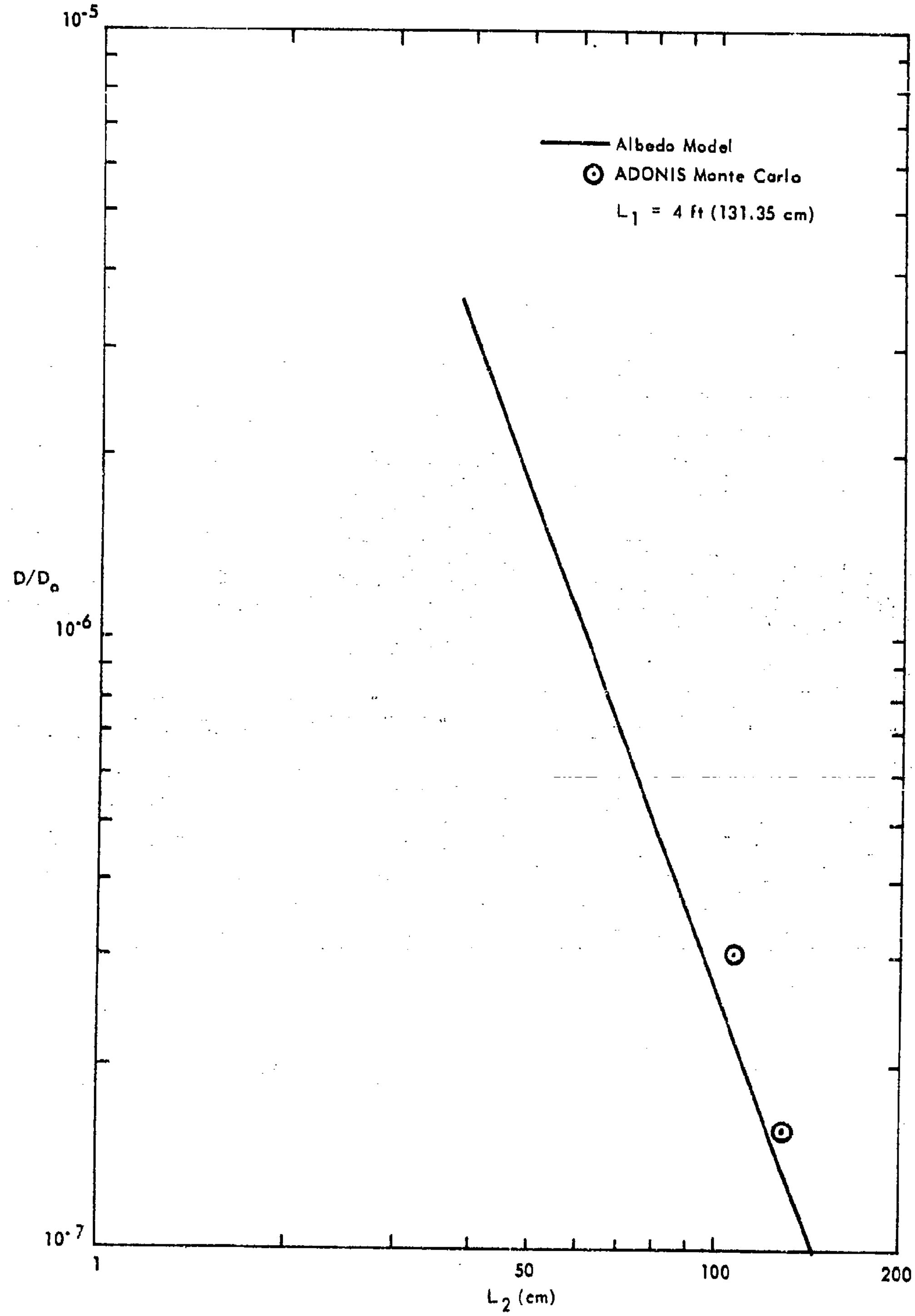

Figure 10. Comparison of albedo model and ADONIS Monte Carlo calculations of T (d, n) reaction in a 11 × 11-inch two-legged duct.

The experimental values[1] and the albedo model calculations for the T (d, n) reaction (14-Mev neutron source) are shown in Figure 11. The geometry of the duct used for the calculations and the experiment was not exactly the same. In the experiment, the source was placed 1 foot outside the entrance of a 15-foot first leg; in the calculations, the source was placed at the entrance of a 16-foot first leg. In this comparison, it is assumed that the geometrical difference of 1 foot in the first leg would not significantly affect the calculated results. As seen in this comparison, the calculated values are slightly lower than the experimental values. Again, this is expected since the higher orders of reflection are neglected in the albedo model calculations.

The experimental values and the albedo model calculations for the D (d, n) reaction (2.5-Mev neutron source) are shown in Figure 12. The ADONIS Monte Carlo calculation required 25 hours of IBM-7090 computer time, while the albedo calculation was performed in 45 minutes on the IBM-1620.

FINDINGS AND CONCLUSIONS

1. Calculations of fast neutron streaming by means of the semiempirical formula developed in this study, based on the albedo concept, are in close agreement with calculations by the ADONIS Monte Carlo technique.

2. Calculation by the semiempirical formula took about one-thirtieth the computer time required for the Monte Carlo method.

3. Agreement between the results of experiments and the theoretical calculations was within 15 percent.

4. For the purpose of obtaining engineering design criteria, it is sufficiently accurate to use the values of the dose distributions in the second leg of the duct which are obtained by albedo model calculations using second-order approximations.

FUTURE PLANS

This was a preliminary study on this subject. In order to have more complete information, it is necessary to study the problem for a variety of duct dimensions. In the near future, an experimental study of corner effects and the effect of duct shape will be compared with the albedo model calculations. Also it is planned to further compare the three independent approaches to this problem: the experimental studies, albedo model calculations, and ADONIS Monte Carlo calculations.

In order to obtain better results with the albedo model calculations, it may be necessary to calculate the higher order reflection contributions to the total dose. However, such calculations are expected to be very difficult and to require lengthy computer computations. In fact, the more accurate high-order calculations may well be prohibitively expensive.

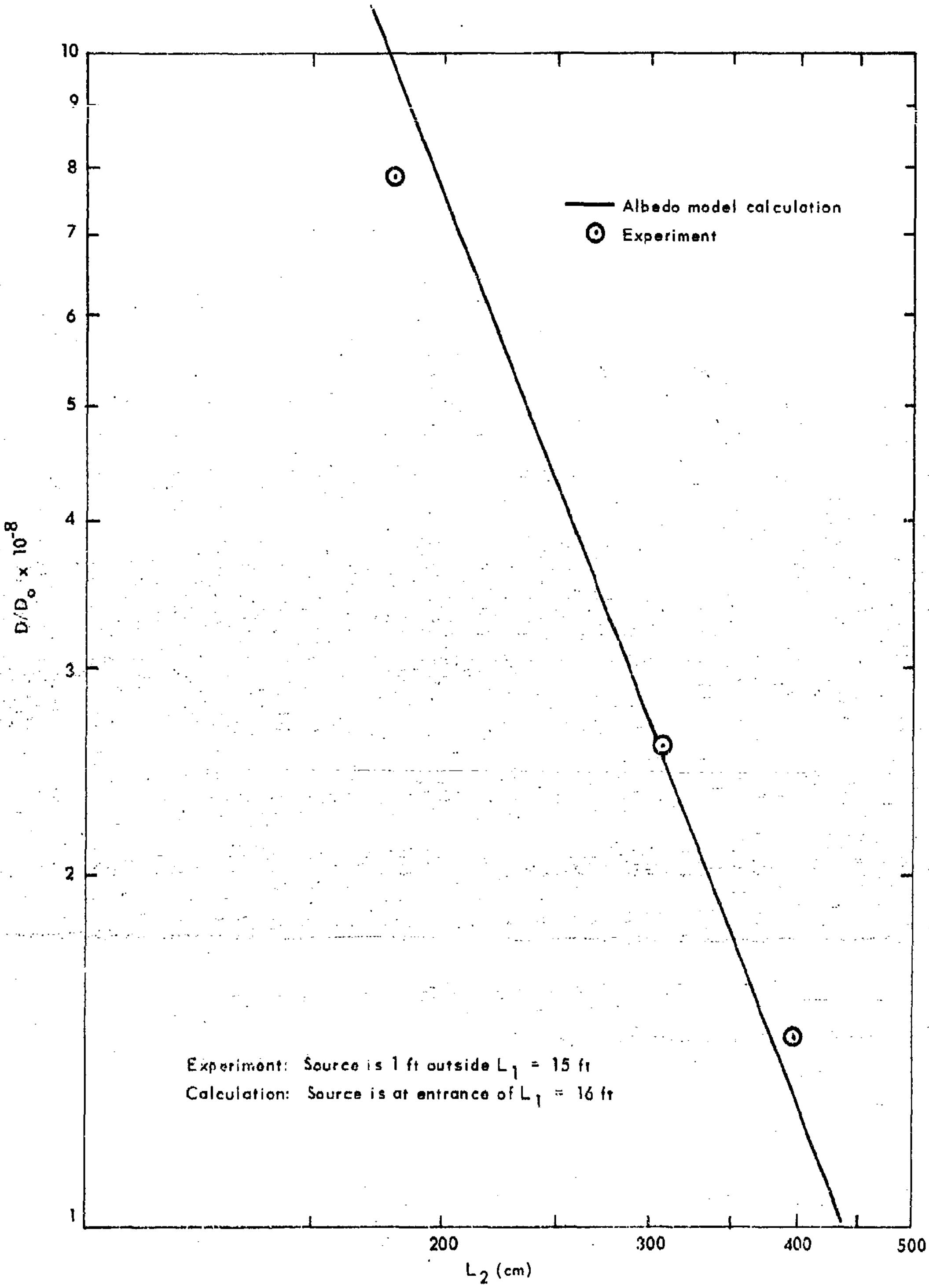

Figure 11. Comparison of albedo model calculation and experimental measurements of T (d, n) reaction in a 3 x 3-foot two-legged duct for a 14-Mev neutron source.

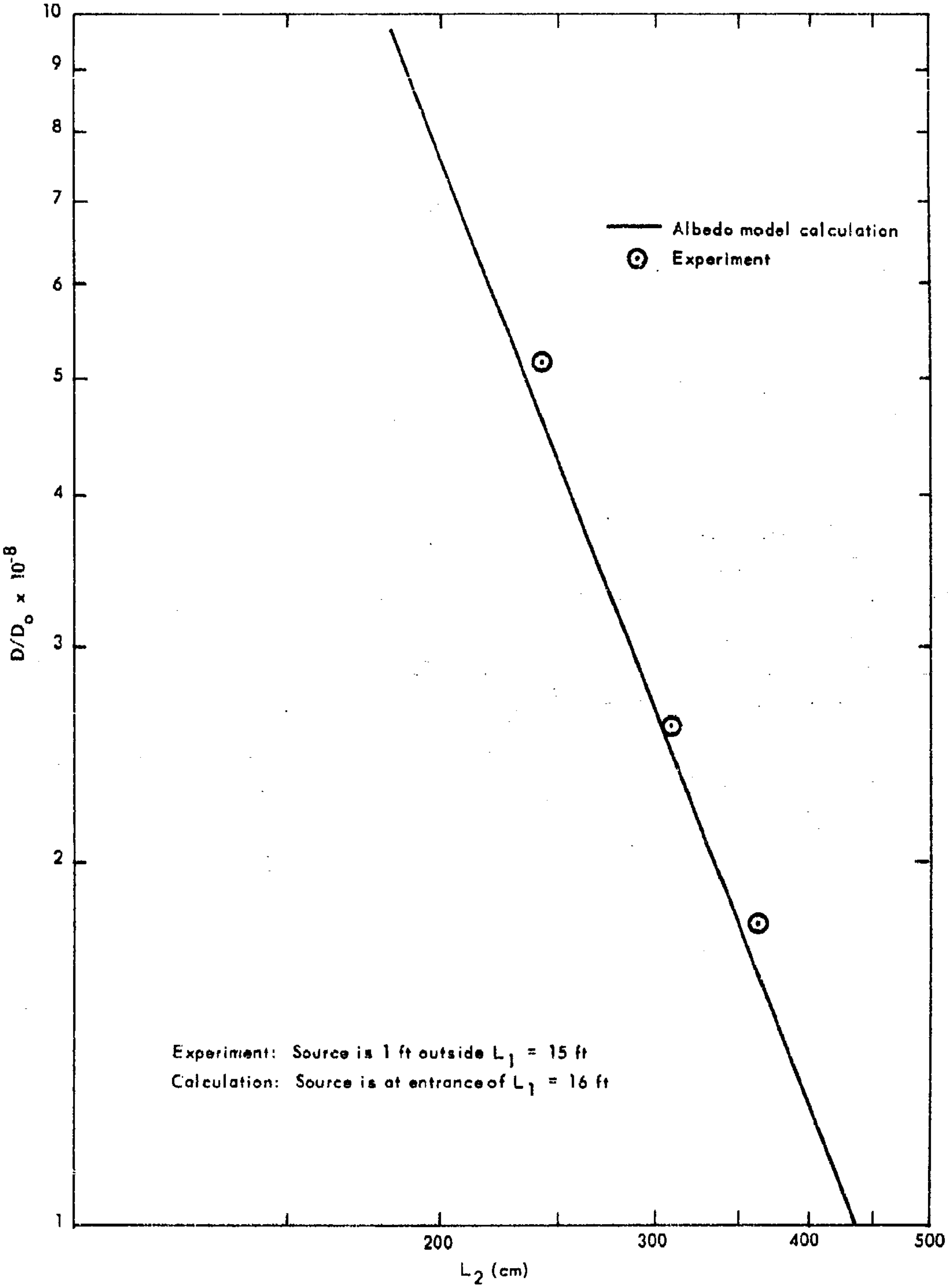

Figure 12. Comparison of albedo model calculation and experimental measurements of D (d, n) reaction in a 3 x 3-foot two-legged duct for a 2.5-Mev neutron source.

Appendix

COMPARISON OF RESULTS OF ONE-PARAMETER FORMULA, SEMIEMPIRICAL FORMULA, AND MONTE CARLO DATA

Dr. L. B. Gardner and Mr. A. J. Mettler of NCEL furnished the results of the Monte Carlo calculations.

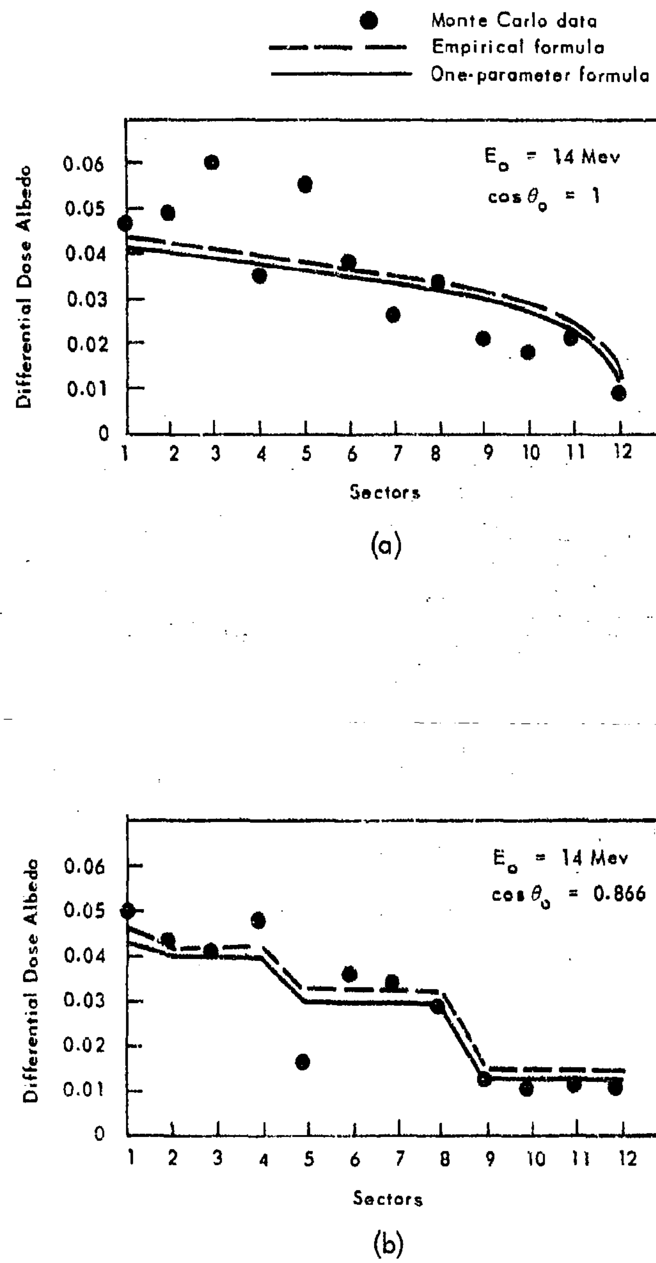

Monte Carlo data
Empirical formula
One-parameter formula
Differential Dose Albedo
0.06
0.05
0.04
0.03
0.02
0.01
0
1
2
3
4
5
6
7
8
9
10
11
12
Sectors
E$_o$ = 14 Mev
cos θ$_o$ = 1
(a)
E$_o$ = 14 Mev
cos θ$_o$ = 0.866
(b)

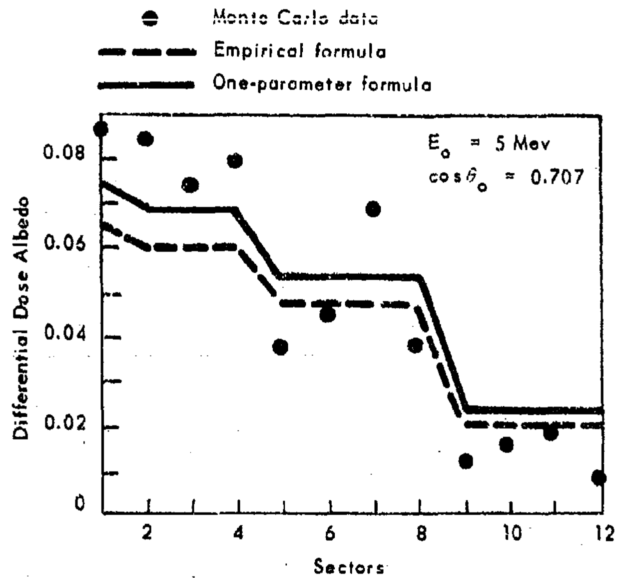

Monte Carlo data
Empirical formula
One-parameter formula
E_o = 5 Mev
$\cos\theta_o$ = 0.707
Differential Dose Albedo
0.08
0.06
0.04
0.02
0
2
4
6
8
10
12
Sectors

(c)

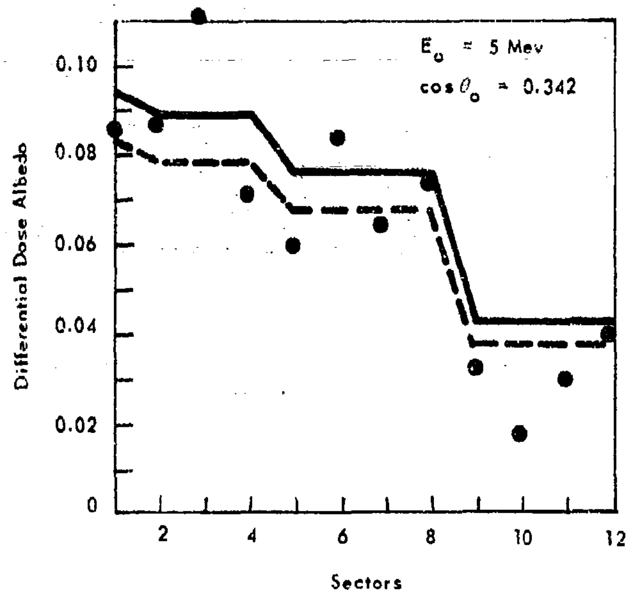

E_o = 5 Mev
$\cos\theta_o$ = 0.342
Differential Dose Albedo
0.10
0.08
0.06
0.04
0.02
0
2
4
6
8
10
12
Sectors

(d)

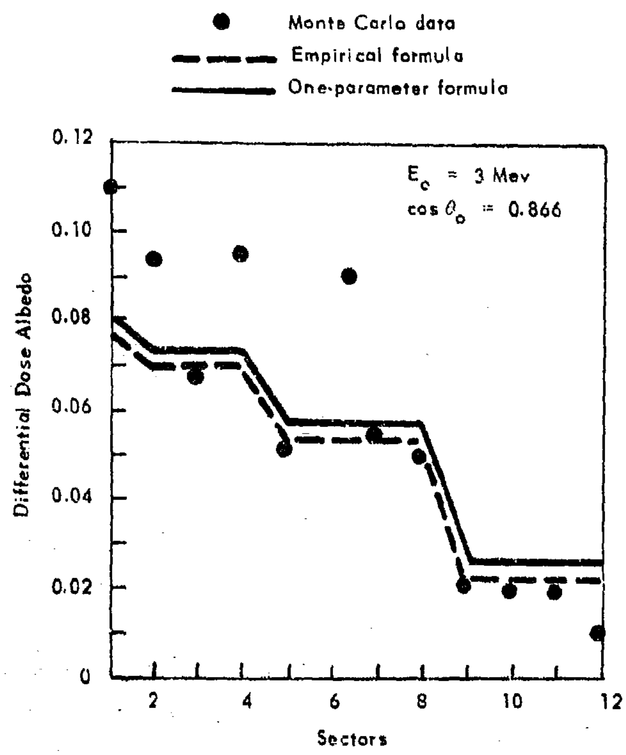
Monte Carlo data
Empirical formula
One-parameter formula
E_o = 3 Mev
cos θ_o = 0.866
Differential Dose Albedo
0.12
0.10
0.08
0.06
0.04
0.02
0
2
4
6
8
10
12
Sectors

(e)

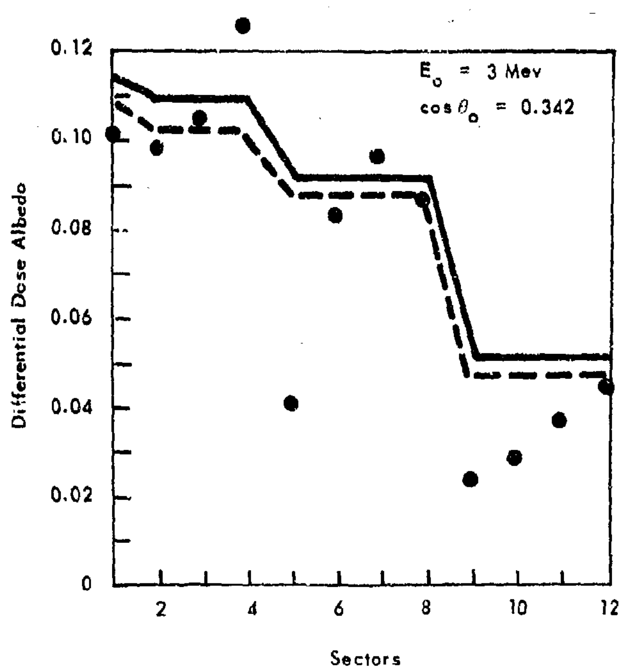
E_o = 3 Mev
cos θ_o = 0.342
Differential Dose Albedo
0.12
0.10
0.08
0.06
0.04
0.02
0
2
4
6
8
10
12
Sectors

(f)

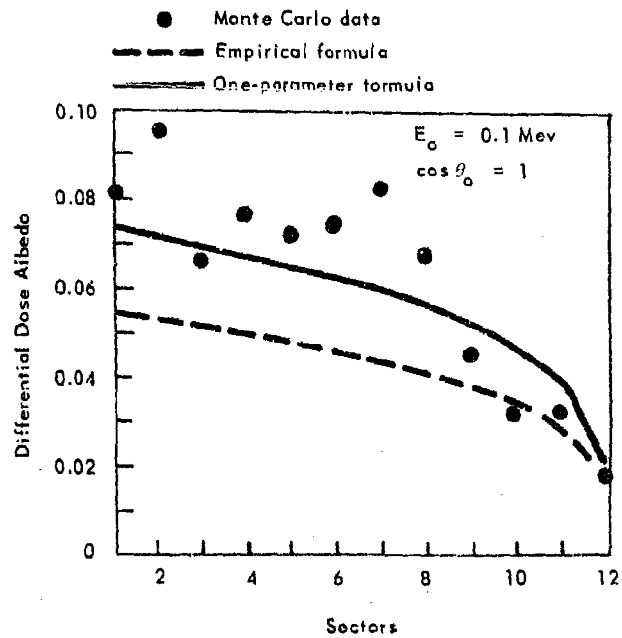
Monte Carlo data
Empirical formula
One-parameter formula
E_o = 0.1 Mev
$\cos \theta_o$ = 1
Differential Dose Albedo
0.10
0.08
0.06
0.04
0.02
0
2
4
6
8
10
12
Sectors

(g)

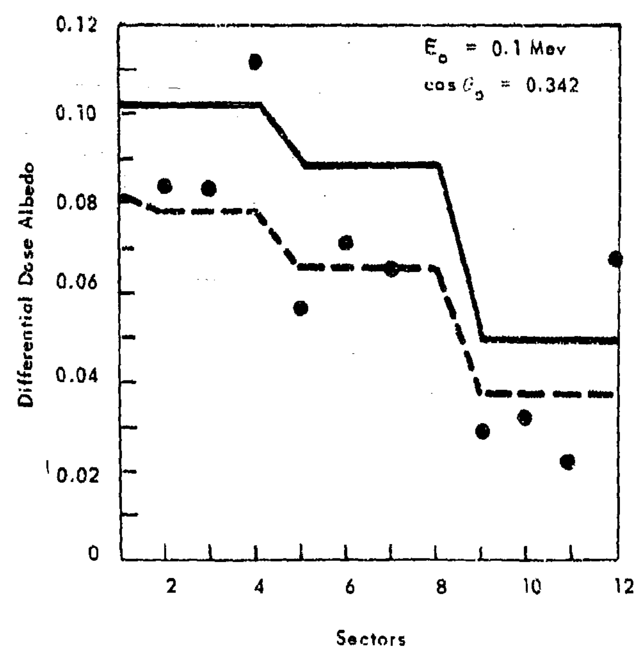
E_o = 0.1 Mev
$\cos \theta_o$ = 0.342
Differential Dose Albedo
0.12
0.10
0.08
0.06
0.04
0.02
0
2
4
6
8
10
12
Sectors

(h)

REFERENCES

1. U. S. Naval Civil Engineering Laboratory. Technical Report R-282: Dose measurements for neutron streaming in ducts, by D. R. Doty. Port Hueneme, Calif., March 1964.

2. A. Simon and C. E. Clifford. The attenuation of neutrons in air ducts in shields, Nuclear Science and Engineering, vol. 1, no. 2, May 1956, pp. 156-166.

3. A. B. Chilton and C. M. Huddleston. A semiempirical formula for differential dose albedo for gamma rays on concrete, Nuclear Science and Engineering, vol. 17, no. 3, Nov. 1963, pp. 419-424.

4. U. S. Army Ballistic Research Laboratories. Report no. 1189: Neutron reflection and flux versus depth for concrete, by Frank J. Allen and others. Aberdeen Proving Ground, Maryland, Jan. 1963.

5. B. Davison and J. B. Sykes. Neutron transport theory. Oxford, Clarendon Press, 1957.

6. U. S. Naval Civil Engineering Laboratory. Technical Report R-264: Computer calculation of dose rates in two-legged ducts using the albedo concept, by J. M. Chapman. Port Hueneme, Calif., Oct. 1963.

7. J. C. LeDoux and A. B. Chilton. Gamma-ray streaming through two-legged rectangular ducts, Nuclear Science and Engineering, vol. 11, no. 4, Dec. 1961, pp. 362-368.

8. United Nuclear Corporation, Development Division-NDA. Report no. UNUCORO635: ADONIS, an IBM-7090 Monte Carlo shielding code which solves for the transport of neutrons or gamma rays in three-dimensional rectangular geometry; vol. 5, Advanced shield calculational techniques, by Barton Eiseman and Elinor Hennessy. White Plains, N. Y., March 1963. Contr. AT(30-1)-2303.

9. Texas Nuclear Corporation. Instruction manual, Model 9120 spherical neutron dosimeter. Austin, Texas, n.d.

DISTRIBUTION LIST

SNDL Code	No. of Activities	Total Copies	
	1	25	Chief, Defense Atomic Support Agency, Washington, D. C.
	1	10	Chief, Bureau of Yards and Docks (Code 42)
23A	1	1	Naval Forces Commanders (Taiwan only)
39B	2	2	Construction Battalions
39D	5	5	Mobile Construction Battalions
39E	3	3	Amphibious Construction Battalions
39F	1	2	Construction Battalion Base Units
A2A	1	1	Chief of Naval Research - Only
A3	2	2	Chief of Naval Operation (OP-07, OP-04)
A5	5	5	Bureaus
B3	2	2	Colleges
E4	1	2	Laboratory ONR (Washington, D. C. only)
E5	1	1	Research Office ONR (Pasadena only)
E16	1	1	Training Device Center
F9	7	7	Station — CNO (Boston; Key West; San Juan; Long Beach; San Diego; Treasure Island; and Rodman, C. Z. only)
F17	6	6	Communication Station (San Juan; San Francisco; Pearl Harbor; Adak, Alaska; and Guam only)
F41	1	1	Security Station
F42	1	1	Radio Station (Oso and Cheltanham only)
F48	1	1	Security Group Activities (Winter Harbor only)
F61	2	2	Naval Support Activities (London and Naples only)
F77	1	1	Submarine Base (Groton, Conn. only)
F81	2	2	Amphibious Bases
H3	7	7	Hospital (Chelsea; St. Albans, Portsmouth, Va., Beaufort; Great Lakes; San Diego, and Camp Pendleton only)
H6	1	1	Medical Center
J1	2	2	Administration Command and Unit — BuPers (Great Lakes and San Diego only)
J3	1	1	U. S. Fleet Anti-Air Warfare Training Center (Virginia Beach only)
J19	1	1	Receiving Station (Brooklyn only)
J34	1	1	Station — BuPers (Washington, D. C. only)

DISTRIBUTION LIST (Cont'd)

SNDL Code	No. of Activities	Total Copies	
J46	1	1	Personnel Center
J48	1	1	Construction Training Unit
J60	1	1	School Academy
J65	1	1	School CEC Officers
J84	1	1	School Postgraduate
J90	1	1	School Supply Corps
J95	1	1	School War College
J99	1	1	Communication Training Center
L1	11	11	Shipyards
L7	4	4	Laboratory – BuShips (New London; Panama City; Cordero and Annapolis only)
L26	5	5	Naval Facilities – BuShips (Antigua; Turks Island, Barbad San Salvador; and Eleuthera only)
L42	2	2	Fleet Activities – BuShips
M27	4	4	Supply Center
M28	6	6	Supply Depot (except Guantanamo Bay; Subic Bay, and Yokos
M61	2	2	Aviation Supply Office
N1	6	18	BuDocks Director, Overseas Division
N2	9	27	Public Works Offices
N5	3	9	Construction Battalion Center
N6	5	5	Construction Officer-in-Charge
N7	1	1	Construction Resident-Officer-in-Charge
N9	6	12	Public Works Center
N14	1	1	Housing Activity
R9	2	2	Recruit Depots
R10	2	2	Supply Installations (Albany and Barstow only)
R20	1	1	Marine Corps Schools (Quantico)
R64	3	3	Marine Corps Base
R66	1	1	Marine Corps Camp Detachment (Tengan only)
W1A1	6	6	Air Station
W1A2	35	35	Air Station
W1B	8	8	Air Station Auxiliary

DISTRIBUTION LIST (Cont'd)

SNDL Code	No. of Activities	Total Copies	
W1C	3	3	Air Facility (Phoenix; Naha; and Naples only)
W1E	6	6	Marine Corps Air Station (except Quantico)
W1H	9	9	Station – BuWeps (except Rota)
	1	1	Deputy Chief of Staff, Research and Development, Headquarters, U. S. Marine Corps, Washington, D. C.
	1	1	President, Marine Corps Equipment Board, Marine Corps School, Quantico, Va.
	1	1	Chief of Staff, U. S. Army, Chief of Research and Development, Department of the Army, Washington, D. C.
	1	1	Office of the Chief of Engineers, Assistant Chief of Engineering for Civil Works, Department of the Army, Washington, D. C.
	1	1	Chief of Engineers, Department of the Army, Washington, D. C., Attn: Engineering Research and Development Division
	1	1	Chief of Engineers, Department of the Army, Washington, D. C., Attn: ENGCW-OE
	1	3	Headquarters, U. S. Air Force, Directorate of Civil Engineering, Washington, D. C., Attn: AFOCE-ES
	1	1	Commanding Officer, U. S. Naval Construction Battalion Center, Port Hueneme, Calif., Attn: Materiel Dept., Code 140
	1	1	Deputy Chief of Staff, Development, Director of Research and Development, Department of the Air Force, Washington, D. C.
	1	1	Director, National Bureau of Standards, Department of Commerce, Connecticut Avenue, Washington, D. C.
	1	2	Office of the Director, U. S. Coast and Geodetic Survey, Washington, D. C.
	1	20	Defense Documentation Center, Building 5, Cameron Station, Alexandria, Va.
	1	2	Director of Defense Research and Engineering, Department of Defense, Washington, D. C.
	1	2	Director, Bureau of Reclamation, Washington, D. C.
	1	1	Facilities Officer, Code 108, Office of Naval Research, Washington, D. C.
	1	1	Federal Aviation Agency, Office of Management Services, Administrative Services Division, Washington, D. C., Attn: Library Branch

DISTRIBUTION LIST (Cont'd)

No. of Activities	Total Copies	
1	2	Commander Naval Beach Group Two, U. S. Naval Amphibious Base, Little Creek, Norfolk, Va.
1	1	Commander, Pacific Missile Range, Technical Documentation Section, P. O. Box 10, Point Mugu, Calif., Attn: Code 4332
1	2	U. S. Army Engineer Research and Development Laboratories, Attn: STINFO Branch, Fort Belvoir, Va.
1	1	Director, U. S. Naval Ordnance Laboratory, White Oak, Silver Springs, Md.
1	1	Office of Naval Research, Branch Office, Navy No. 100, Box 39, FPO, New York
1	1	U. S. Naval Radiological Defense Laboratory, San Francisco
1	1	Officer in Charge, CECOS, Port Hueneme, Calif., Attn: ADCE Course
1	1	U. S. Air Force, Asst. Chief of Staff, Intelligence, Building B, AHS, Washington, D. C., Attn: Mr. Sargent White
1	1	Commander, Space Systems Division, Los Angeles Air Force Station, Los Angeles, Calif., Attn: SSSD
1	1	Directorate of Research, Air Force Weapons Laboratory, Kirtland Air Force Base, N. M.
1	1	Office of the Chief of Engineers, Department of the Army, T-7, Gravelly Point, Washington, D. C., Attn: ENGNB
1	1	Commanding Officer, Engineer Research and Development Laboratories, Fort Belvoir, Va.
1	1	Office of the Chief of Engineers, Department of the Army, T-7, Gravelly Point, Washington, D. C., Attn: ENG MC-EB
1	1	Director, U. S. Army Engineer Waterways Experiment Station, P. O. Box 631, Vicksburg, Miss., Attn: Mr. G. L. Arbuthnot, Jr.
1	1	U. S. Army Chemical Center, Nuclear Defense Laboratory, Edgewood, Md.
1	1	Director, Ballistic Research Laboratories, Aberdeen, Md.
1	2	Chief, Defense Atomic Support Agency, Washington, D. C.
1	1	Headquarters, Field Command, Defense Atomic Support Agency, Sandia Base, Albuquerque, N. M.
1	1	U. S. Atomic Energy Commission, Technical Information Service, P. O. Box 62, Oak Ridge, Tenn.
1	1	Director, Civil Effects Test Group, Atomic Energy Commission, Washington, D. C.
1	1	Formulation and Analysis Branch, Mathematics and Computation Laboratory, National Resource Evaluation Center, Office of Emergency Planning, Washington, D. C.
1	2	Library of Congress, Washington, D. C.

DISTRIBUTION LIST (Cont'd)

No. of Activities	Total Copies	
1	1	Disaster Recovery Training Officer, Code 450, Construction Battalion Center, Davisville, R. I.
1	1	Mr. William J. Taylor, Terminal Ballistics Laboratory, Aberdeen Proving Ground, Md.
1	1	LCDR Charles W. Gulick, Jr., CEC, USN, Navy No. 926, FPO, San Francisco
1	1	CDR J. C. LeDoux, Bureau of Yards and Docks, Department of Navy, Washington, D. C.
1	1	CAPT W. M. McLellon, CEC, USN, Ret., 468 1st Street, Albany, N. Y.
1	1	LT Edward S. Perry, U. S. Naval Reserve Officers Training Corps Unit, University of Illinois, Urbana, Ill.
1	1	CAPT L. N. Saunders, CEC, USN, Code C10, U. S. Naval Construction Battalion Center, Port Hueneme, Calif.
1	1	CDR E. M. Saunders, CEC, USN, Chief of Naval Materiel, Department of the Navy, Washington, D. C.
1	1	CDR R. C. Vance, CEC, USN, Logistics Director, U. S. Naval Civil Engineering Laboratory, Port Hueneme, Calif.
1	1	CDR W. A. Walls, CEC, USN, Disaster Control Division, Bureau of Yards and Docks, Washington, D. C.
1	1	LT COL Charles D. Daniel, USA, Defense Atomic Support Agency, Washington, D. C.
1	1	Mr. L. Neal FitzSimons, Office of Civil Defense, Department of Defense, Washington, D. C.
1	1	Mr. Ben Taylor, Office of Civil Defense, Department of Defense, Washington, D. C.
1	1	Mr. Charles M. Eisenhauer, Radiation Physics Laboratory, National Bureau of Standards, Washington, D. C.
1	1	Mr. O. H. Hill, Building 12, Room 505, Radiation Physics Division, National Bureau of Standards, Washington, D. C.
1	1	CDR J. D. Andrews, CEC, USN, Executive Officer, U. S. Naval Civil Engineering Laboratory, Port Hueneme, Calif.
1	1	CAPT W. J. Christensen, CEC, USN, Commanding Officer and Director, U. S. Naval Civil Engineering Laboratory, Port Hueneme, Calif.
1	1	CDR J. F. Dobson, CEC, USN, Office of Civil Defense, Department of Army, Washington, D. C.
1	1	LCDR O. L. Dixon, CEC, USN, U. S. Naval School, CEC Officers, Port Hueneme, Calif.
1	1	LCDR N. W. Clements, CEC, USN, Navy Nuclear Power Unit, Fort Belvoir, Va.
1	1	CDR C. Curione, CEC, USN, Resident Officer-In-Charge-Of-Construction, Long Beach Area, P.O. Box XX, Seal Beach, Calif.

DISTRIBUTION LIST (Cont'd)

No. of Activities	Total Copies	
1	1	LCDR T. Yoshihara, CEC, USN, ROICC, Southeast Asia, APO 143, San Francisco
1	1	LT L. K. Donovan, CEC, USN, U. S. Naval Communication Station, Navy No. 85, FPO, San Francisco
1	1	LCDR Walter J. Eager, Jr., CEC, USN, AFRRI-NNMC, Bethesda, Md.
1	1	CDR W. J. Francy, CEC, USN, United States Naval Academy, Annapolis, Md.
1	1	Dr. Lauriston S. Taylor, Chief, Radiation Physics Division, National Bureau of Standards, Washington, D. C.
1	1	Dr. James O. Buchanan, Research Directorate, Office of Civil Defense, Washington, D. C.
1	1	Mr. Jack C. Greene, Office of Civil Defense, Department of Defense, Washington, D. C.
1	1	Dr. Harold A. Knapp, Fallout Studies Branch, Division of Biology and Medicine, U. S. Atomic Energy Commission, Washington, D. C.
1	1	Dr. Karl Z. Morgan, Director, Health Physics Division, Oak Ridge National Laboratory, Oak Ridge, Tenn.
1	1	Dr. Joseph D. Coker, National Resource Evaluation Center, Executive Office Building, Washington, D. C.
1	1	Dr. Charles F. Ksanda, Military Evaluation Division, U. S. Naval Radiological Defense Laboratory, San Francisco
1	1	Mr. John Auxier, Oak Ridge National Laboratory, Oak Ridge, Tenn.
1	1	Dr. William Kreger, Naval Radiological Defense Laboratory, San Francisco
1	1	Dr. Hans Tiller, Nuclear Defense Laboratory, Army Chemical Center, Md.
1	1	Mr. Irving Gaskill, National Resource Evaluation Center, Executive Office Building, Washington, D. C.
1	1	Mr. George Sisson, Office of Civil Defense, Department of Defense, Washington, D. C.
1	1	Mr. James C. Pettee, National Resource Evaluation Center, Executive Office Building, Washington, D. C.
1	1	LCDR I. D. Crawley, CEC, USN, Blast and Shock Division, Defense Atomic Support Agency, Washington, D. C.
1	1	CAPT H. L. Murphy, Room 211, Federal Office Building, San Francisco
1	1	LCDR W. H. Bannister, CEC, USN, Field Command, Defense Atomic Support Agency, Sandia Base, Albuquerque, N. M.
1	1	Major Robert Crawford, USAF, Air Force Weapons Laboratory, Kirtland Air Force Base, Albuquerque, N. M.
1	1	Dr. John Balloch, Director, Operations Analysis, 26th Air Division, SAGE, Hancock Field, Syracuse, N. Y.

DISTRIBUTION LIST (Cont'd)

No. of Activities	Total Copies	
1	1	Mr. J. F. Tamonini, A & E Development Division, Office of Civil Defense, Department of Defense, Washington, D. C.
1	1	CDR C. R. Whipple, CEC, USN, Armed Forces Staff College, Norfolk, Va.
1	1	Dr. W. E. Fisher, Air Force Weapons Laboratory, Kirtland Air Force Base, Albuquerque, N. M.
1	1	Mr. Everitt P. Blizard, Director, Neutron Physics, Oak Ridge National Laboratory, P. O. Box X, Oak Ridge, Tenn.
1	1	LT M. MacDonald, CEC, USN, U. S. Naval School, CEC Officers, Port Hueneme, Calif.
1	1	Library, Engineering Department, University of California, 405 Hilgard Avenue, Los Angeles
1	1	Sandia Corporation, Box 5800, Albuquerque, N. M.
1	1	Rivers and Harbor Library, Princeton University, Princeton, N. J.
1	1	Head, Civil Engineering Department, Carnegie Institute of Technology, Schenley Park, Pittsburgh, Pa.
1	1	Mr. G. H. Albright, Head, Department of Architectural Engineering, 101 Engineering "A" Bldg., The Pennsylvania State University, University Park, Pa
1	1	Dr. N. M. Newmark, Civil Engineering Hall, University of Illinois, Urbana, Ill.
1	1	Professor J. Neils Thompson, Civil Engineering Department, University of Texas, Austin, Tex.
1	1	Mr. Fred Sauer, Physics Department, Stanford Research Institute, Menlo Park, Calif.
1	1	Dr. T. H. Schiffman, Armour Research Foundation of Illinois, Institute of Technology, Technology Center, Chicago, Ill.
1	1	Dr. Robert V. Whitman, Massachusetts Institute of Technology, Cambridge, Mass.
1	1	Dr. Lewis V. Spencer, Ottawa University, Physics Department, Ottawa, Kan.
1	1	Mr. E. E. Shalowitz, Protective Construction, GSA Building, 19th and F Streets, N. W., Washington, D. C.
1	1	Mr. Werner Weber, Nuclear Engineering Consultant, N. Y. State Civil Defense Commission, P. O. Box 7007, State Office Building, Albany, N. Y.
1	1	Dr. Harold Brode, The Rand Corporation, 1700 Main Street, Santa Monica, Calif.
1	1	Mr. R. D. Cavanaugh, Barry Controls, Inc., 700 Pleasant Street, Watertown, Mass.
1	1	Mr. Kenneth Kaplan, Broadview Research Corporation, 1811 Trousdale Drive, Burlingame, Calif.
1	1	Mr. Thomas Morrison, American Machine and Foundry Company, 7501 North Natchez Avenue, Niles, Ill.

DISTRIBUTION LIST (Cont'd)

No. of Activities	Total Copies	
1	1	Mr. Walter Gunther, The Mitre Corporation, P. O. Box 208, Lexington, Mass.
1	1	Mr. W. R. Perret – 5112, Applied Experiments Division, Sandia Corporation, Albuquerque, N. M.
1	1	Mr. Lyndon Welch, Eberle M. Smith Associates, Inc., 153 East Elizabeth Street, Detroit, Mich.
1	1	Professor Herbert M. Bosch, Public Health Engineering, School of Public Health, University of Minnesota, Minneapolis, Minn.
1	1	Dr. Merit P. White, Civil Engineering Department, School of Engineering, University of Massachusetts, Amherst, Mass.
1	1	Dr. Robert J. Hansen, Department of Civil & Sanitary Engineering, Massachusetts Institute of Technology, Cambridge, Mass.
1	1	Mr. Harold Horowitz, Building Research Institute, National Academy of Sciences, 2101 Constitution Avenue, N. W., Washington, D. C.
1	1	Mr. Luke Vortman – 5112, Applied Experiments Division, Sandia Corporation, Albuquerque, N. M.
1	1	Mr. Richard Park, National Academy of Sciences, 2101 Constitution Avenue, N. W., Washington, D. C.
1	1	Mr. Frederick A. Pawley, AIA Research Secretary, American Institute of Architects, 1735 New York Avenue, N. W., Washington, D. C.
1	1	Dr. E. E. Massey, Defense Research Board, Department of National Defense, Ottawa, Canada
1	1	Dr. Robert Rapp, The Rand Corporation, 1700 Main Street, Santa Monica, Calif.
1	1	Dr. Stephen B. Withey, Program Director, Survey Research Center, University of Michigan, Ann Arbor, Mich.
1	1	Dr. Eric T. Clarke, Technical Operations, Inc., Burlington, Mass.
1	1	Dr. A. B. Chilton, Civil Engineering Hall, University of Illinois, Urbana, Ill.
1	1	Mrs. Shea Valley, CRTZS, A. F. Cambridge Research Center, L. G. Hanscom Field, Bedford, Mass.
1	1	Dr. J. T. Hanley, Department of Civil Engineering, University of Minnesota, Minneapolis, Minn.
1	1	Professor J. Silverman, Department of Chemical Engineering, University of Maryland, College Park, Md.
1	1	Dr. F. T. Mavis, Dean, College of Engineering, University of Maryland, College Park, Md.
1	1	Dr. Raymond R. Fox, Associate Professor and Director, Protective Construction Courses, The George Washington University, Washington, D. C.

DISTRIBUTION LIST (Cont'd)

No. of Activities	Total Copies	
1	1	Chief, Bureau of Ships, Attn: Chief of Research and Development Division, Navy Department, Washington, D. C.
1	1	Officer in Charge, U. S. Naval Biological Laboratory, Naval Supply Center, Oakland, Calif.
1	1	Officer in Charge, U. S. Navy Unit, Rensselaer Polytechnic Institute, Troy, N. Y.
1	1	Chief, Bureau of Medicine and Surgery, Attn: Research Division, Navy Department, Washington, D. C.
1	1	Officer in Charge, U. S. Naval Supply Research and Development Facility, Naval Supply Center, Attn: Library, Bayonne, N. J.
1	1	Director, Marine Physical Laboratory, U. S. Navy Electronics Laboratory, San Diego, Calif.
1	1	Chief, Bureau of Naval Weapons, Attn: Research Division, Navy Department, Washington, D. C.
1	1	Commander, Pacific Missile Range, Attn: Technical Director, Point Mugu, Calif.
1	1	Officer in Charge, U. S. Naval Supply Research and Development Facility, Naval Supply Center, Bayonne, N. J.
1	1	Commander, Norfolk Naval Shipyard, Attn: Chemical Laboratory, Portsmouth, Va.
1	1	Commanding Officer, Fleet Training Center, Navy No. 128, FPO, San Francisco, Calif.
1	1	Commander, U. S. Naval Shipyard, Attn: Rubber Laboratory, Mare Island, Vallejo, Calif.
1	1	Commander, U. S. Naval Shipyard, Attn: Material Laboratory, Brooklyn 1, N. Y.
1	1	Office of Naval Research, Branch Office, Navy No. 100, Box 39, FPO, N. Y.
1	1	Commanding Officer, Naval Electronics Laboratory, Attn: Technical Director, San Diego, Calif.
1	1	Commanding Officer, U. S. Naval Unit, U. S. Army Chemical Corps School, Fort McClellan, Ala.
1	1	U. S. Naval Research Laboratory, Chemistry Division, Washington, D. C.
1	1	Commanding Officer, Field Research Laboratory, Bureau of Medicine and Surgery, Camp Lejeune, N. C.
1	1	Deputy Chief of Staff, Research & Development Headquarters, U. S. Marine Corps, Washington, D. C.
1	1	Commanding Officer, Signal Corps Engineering Labs, Fort Monmouth, N. J.
1	1	Directorate of Medical Research, Chemical Warfare Laboratory, Army Chemical Center, Md.
1	1	U. S. Army Cold Regions Research and Engineering Laboratory, Corps of Engineers, P. O. Box 282, Hanover, N. H.

DISTRIBUTION LIST (Cont'd)

No. of Activities	Total Copies	
1	1	Coles Signal Laboratory, Red Bank, N. J.
1	1	Air Force Cambridge Research Center, Hunscom Field, Mass.
1	1	Directorate of Research, Air Force Special Weapons Center, Kirtland Air Force Base, N. M.
1	1	Arctic Aeromedical Laboratory, United States Air Force, APO 731, Seattle, Wash.
1	1	Commanding Officer, Biological Warfare Laboratories, Fort Detrick, Frederick, Md.
1	1	Sandia Corporation, Attn: Classified Document Division, Box 5800, Albuquerque, N. M.
1	1	Chief, Physical Research Branch, Research Division, U. S. Department of Commerce, Bureau of Public Roads, Washington, D. C.
1	1	Department of Zoology, Duke University, Durham, N. Car.
1	1	Director, Engineering Research Institute, University of Michigan, Ann Arbor, Mich.
1	1	Director, Marine Laboratory, University of Miami, Coral Gables, Fla.
1	1	Director, Soil Physics Laboratory, Department of Engineering, Princeton University, Princeton University, Princeton, N. J.
1	1	Director, The Technological Institution, Northwestern University, Evanston, Ill.
1	1	John F. Batter, CONESCO, Inc., 205 Sixth Street, Cambridge, Mass.
1	1	Prof. D. W. Green, 1668 Maple Avenue, Galesburg, Ill.
1	1	John H. Hubbell, National Bureau of Standards, Washington, D. C.
1	1	Robert M. Kinkaid, Edgerton, Germeshausen, and Greer, Inc., P. O. Box 1912, Las Vegas, Nev.
1	1	Dr. R. L. Ashley, Atomics International, P. O. Box 309, Canoga Park, Calif.
1	1	Ballistic Research Laboratories, Director, Aberdeen, Md.
1	1	Civil Effects Test Group, Director, Atomic Energy Commission, Washington, D. C.
1	1	Library, University of Alaska, Fairbanks, Alaska
1	1	Library, Battelle Institute, Columbus, Ohio
1	1	Library, University of Southern California, University Park, Los Angeles, Calif.
1	1	Library, Institute of Technology, University of Minnesota, Minneapolis, Minn.
1	1	Library, California Institute of Technology, Pasadena, Calif.
1	1	Dr. H. E. Stanton, Physics Division, Argonne National Laboratory, Argonne, Ill.
1	1	Dr. C. W. Terrell, Armour Research Foundation, 10 West 35th Street, Chicago, Ill.
1	1	S. K. Penny, Radiation Shielding Information Center, Oak Ridge National Laboratory, P. O. Box X, Oak Ridge, Tenn.

No. of Activities	Total Copies	
1	1	Professor M. L. P. Go, Civil Engineering Department, University of Hawaii, Honolulu, Hawaii
1	1	Dr. James P. Romualdi, Department of Civil Engineering, Carnegie Institute of Technology, Pittsburg, Pa.
1	1	Dr. Nicholas Perrone, Structural Mechanics Branch, Office of Naval Research, Department of the Navy, Washington , D. C.
1	1	Dr. Aleksandar Sedmak Vesić, Professor of Civil Engineering, College of Engineering, Duke University, Durham, N. C.
1	1	Mr. C. C. Mow, The Rand Corporation, 1700 Main Street, Santa Monica, Calif.
1	1	Systems Engineering Group, Deputy for Systems Engineering, Directorate of Technical Publications and Specifications, Wright-Patterson AFB, Ohio
1	1	Dr. William L. White, Stanford Research Institute, Menlo Park, Calif.
1	1	CDR Allen F. Dill, CEC, USNR, Public Works Officer, Headquarters Support Activity, Taipei, Box 25, APO 63, San Francisco
1	1	Library, Civil Engineering Dept., University of Hawaii, Honolulu, Hawaii

U. S. Naval Civil Engineering Laboratory
FAST NEUTRON STREAMING THROUGH TWO-LEGGED CONCRETE DUCTS, by Y. T. Song

TR-354 | 49 p. illus | 2 Feb 65 | Unclassified

1. Shelters — Neutron streaming
2. Radiation — Neutron streaming

I. Y-F008-08-05-201
II. DASA-11.026

As a part of the Laboratory's fundamental shielding studies for personnel shelters, fast neutron dose rates are calculated in the second leg of an air duct through concrete for neutron energies of 14 Mev and 2.5 Mev. The calculational technique is based on the albedo concept. Dose rates are also calculated by a Monte Carlo technique, and the results obtained by the two theoretical methods are compared with each other and with experimental measurements.

Comparison shows very good agreement among these three independent determinations.

U. S. Naval Civil Engineering Laboratory
FAST NEUTRON STREAMING THROUGH TWO-LEGGED CONCRETE DUCTS, by Y. T. Song

TR-354 | 49 p. illus | 2 Feb 65 | Unclassified

1. Shelters — Neutron streaming
2. Radiation — Neutron streaming

I. Y-F008-08-05-201
II. DASA-11.026

As a part of the Laboratory's fundamental shielding studies for personnel shelters, fast neutron dose rates are calculated in the second leg of an air duct through concrete for neutron energies of 14 Mev and 2.5 Mev. The calculational technique is based on the albedo concept. Dose rates are also calculated by a Monte Carlo technique, and the results obtained by the two theoretical methods are compared with each other and with experimental measurements.

Comparison shows very good agreement among these three independent determinations.

U. S. Naval Civil Engineering Laboratory
FAST NEUTRON STREAMING THROUGH TWO-LEGGED CONCRETE DUCTS, by Y. T. Song

TR-354 | 49 p. illus | 2 Feb 65 | Unclassified

1. Shelters — Neutron streaming
2. Radiation — Neutron streaming

I. Y-F008-08-05-201
II. DASA-11.026

As a part of the Laboratory's fundamental shielding studies for personnel shelters, fast neutron dose rates are calculated in the second leg of an air duct through concrete for neutron energies of 14 Mev and 2.5 Mev. The calculational technique is based on the albedo concept. Dose rates are also calculated by a Monte Carlo technique, and the results obtained by the two theoretical methods are compared with each other and with experimental measurements.

Comparison shows very good agreement among these three independent determinations.

U. S. Naval Civil Engineering Laboratory
FAST NEUTRON STREAMING THROUGH TWO-LEGGED CONCRETE DUCTS, by Y. T. Song

TR-354 | 49 p. illus | 2 Feb 65 | Unclassified

1. Shelters — Neutron streaming
2. Radiation — Neutron streaming

I. Y-F008-08-05-201
II. DASA-11.026

As a part of the Laboratory's fundamental shielding studies for personnel shelters, fast neutron dose rates are calculated in the second leg of an air duct through concrete for neutron energies of 14 Mev and 2.5 Mev. The calculational technique is based on the albedo concept. Dose rates are also calculated by a Monte Carlo technique, and the results obtained by the two theoretical methods are compared with each other and with experimental measurements.

Comparison shows very good agreement among these three independent determinations.

Unclassified

Security Classification

DOCUMENT CONTROL DATA · R&D

(Security classification of title, body of abstract and indexing annotation must be entered when the overall report is classified)

1. ORIGINATING ACTIVITY (Corporate author) U. S. Naval Civil Engineering Laboratory Port Hueneme, California 93041	2a. REPORT SECURITY CLASSIFICATION Unclassified 2b. GROUP

3. REPORT TITLE

Fast Neutrons Streaming Through Two-Legged Concrete Ducts

4. DESCRIPTIVE NOTES (Type of report and inclusive dates)

Preliminary study February 1964 - September 1964

5. AUTHOR(S) (Last name, first name, initial)

Song, Y. T.

6. REPORT DATE	7a. TOTAL NO. OF PAGES	7b. NO. OF REFS
2 February 1965	49	9

8a. CONTRACT OR GRANT NO. DASA — 11.026	9a. ORIGINATOR'S REPORT NUMBER(S)
b. PROJECT NO. Y-F008-08-05-201	TR-354
c.	9b. OTHER REPORT NO(S) (Any other numbers that may be assigned this report)
d.	

10. AVAILABILITY/LIMITATION NOTICES

Qualified requesters may obtain copies of this report from DDC.

11. SUPPLEMENTARY NOTES	12. SPONSORING MILITARY ACTIVITY
	DASA — BUDOCKS

13. ABSTRACT

As a part of the Laboratory's fundamental shielding studies for personnel shelters, fast neutron dose rates are calculated in the second leg of an air duct through concrete for neutron energies of 14 Mev and 2.5 Mev. The calculational technique is based on the albedo concept. Dose rates are also calculated by a Monte Carlo technique, and the results obtained by the two theoretical methods are compared with each other and with experimental measurements.

Comparison shows very good agreement among these three independent determinations.

Unclassified

Security Classification

14. KEY WORDS	LINK A ROLE	LINK A WT	LINK B ROLE	LINK B WT	LINK C ROLE	LINK C WT
Formulas	8					
Computation	4,8					
Fast Neutrons	9					
Radiation	9					
Dosage	9					
Ducts	9					
Shelters	9					
Subsurface Structures	9					
Radiation Shielding	4					

INSTRUCTIONS

1. ORIGINATING ACTIVITY: Enter the name and address of the contractor, subcontractor, grantee, Department of Defense activity or other organization *(corporate author)* issuing the report.

2*a*. REPORT SECURITY CLASSIFICATION: Enter the overall security classification of the report. Indicate whether "Restricted Data" is included. Marking is to be in accordance with appropriate security regulations.

2*b*. GROUP: Automatic downgrading is specified in DoD Directive 5200.10 and Armed Forces Industrial Manual. Enter the group number. Also, when applicable, show that optional markings have been used for Group 3 and Group 4 as authorized.

3. REPORT TITLE: Enter the complete report title in all capital letters. Titles in all cases should be unclassified. If a meaningful title cannot be selected without classification, show title classification in all capitals in parenthesis immediately following the title.

4. DESCRIPTIVE NOTES: If appropriate, enter the type of report, e.g., interim, progress, summary, annual, or final. Give the inclusive dates when a specific reporting period is covered.

5. AUTHOR(S): Enter the name(s) of author(s) as shown on or in the report. Enter last name, first name, middle initial. If military, show rank and branch of service. The name of the principal author is an absolute minimum requirement.

6. REPORT DATE: Enter the date of the report as day, month, year; or month, year. If more than one date appears on the report, use date of publication.

7*a*. TOTAL NUMBER OF PAGES: The total page count should follow normal pagination procedures, i.e., enter the number of pages containing information.

7*b*. NUMBER OF REFERENCES: Enter the total number of references cited in the report.

8*a*. CONTRACT OR GRANT NUMBER: If appropriate, enter the applicable number of the contract or grant under which the report was written.

8*b*, 8*c*, & 8*d*. PROJECT NUMBER: Enter the appropriate military department identification, such as project number, subproject number, system numbers, task number, etc.

9*a*. ORIGINATOR'S REPORT NUMBER(S): Enter the official report number by which the document will be identified and controlled by the originating activity. This number must be unique to this report.

9*b*. OTHER REPORT NUMBER(S): If the report has been assigned any other report numbers *(either by the originator or by the sponsor)*, also enter this number(s).

10. AVAILABILITY/LIMITATION NOTICES: Enter any limitations on further dissemination of the report, other than those imposed by security classification, using standard statements such as:

(1) "Qualified requesters may obtain copies of this report from DDC."

(2) "Foreign announcement and dissemination of this report by DDC is not authorized."

(3) "U. S. Government agencies may obtain copies of this report directly from DDC. Other qualified DDC users shall request through ________________."

(4) "U. S. military agencies may obtain copies of this report directly from DDC. Other qualified users shall request through ________________."

(5) "All distribution of this report is controlled. Qualified DDC users shall request through ________________."

If the report has been furnished to the Office of Technical Services, Department of Commerce, for sale to the public, indicate this fact and enter the price, if known.

11. SUPPLEMENTARY NOTES: Use for additional explanatory notes.

12. SPONSORING MILITARY ACTIVITY: Enter the name of the departmental project office or laboratory sponsoring *(paying for)* the research and development. Include address.

13. ABSTRACT: Enter an abstract giving a brief and factual summary of the document indicative of the report, even though it may also appear elsewhere in the body of the technical report. If additional space is required, a continuation sheet shall be attached.

It is highly desirable that the abstract of classified reports be unclassified. Each paragraph of the abstract shall end with an indication of the military security classification of the information in the paragraph, represented as *(TS)*, *(S)*, *(C)*, or *(U)*.

There is no limitation on the length of the abstract. However, the suggested length is from 150 to 225 words.

14. KEY WORDS: Key words are technically meaningful terms or short phrases that characterize a report and may be used as index entries for cataloging the report. Key words must be selected so that no security classification is required. Identifiers, such as equipment model designation, trade name, military project code name, geographic location, may be used as key words but will be followed by an indication of technical context. The assignment of links, roles, and weights is optional.

Unclassified

Security Classification